People's Democratic Republic of Algeria

Ministry of Higher Education and Scientific Research

University M'Hamed BOUGARA - Boumerdes

Institute of Electrical and Electronic Engineering

Department of Electronics

Final Year Project Report Presented in Partial Fulfillment of the Requirements for the Degree of

MASTER

In **Power Engineering**

Option: **Power Engineering**

Title

Identification of PV model parameters using experimental and nameplate data

Presented by:

- Mr. Atchi Aymene

- Ms. Khaled Rayane

Supervisor:

Prof. Aissa KHELDOUN

Abstract

In the last few decades, the use of photovoltaic systems has enormously increased. Hence tools to predict energy production are highly needed. This work presents two reliable methods for identifying the optimal parameters of a PV generating unit. In the first method, the PV system is simulated using single and double diode models. It is based on an opposition-based differential evolution algorithm where the objective function is derived from the experimental current-voltage data. In the second method, the parameters of the single diode model are identified using only datasheets provided by manufacturers. It is based on a new meta-heuristics method called Black Widow. These methods are found to be useful for designers since they are simple, fast, and accurate. The analysis is performed on different PV cells/modules and under different temperatures and irradiances. The final results are compared with different existing methods.

Acknowledgments

Praise to Allah, the supreme for leading us in our study path, and for allowing us to realize this work.

We would like to thank our families for their continued support, especially our parents who never stopped helping and encouraging us through our academic years.

Our deep gratitude and thanks go to:

Prof. Kheldoun, our teacher and supervisor who taught us the basics of power systems through these two years and developed our interest for this field besides instructed us the necessary knowledge to accomplish this work.

We acknowledge with much appreciation the jury members for having honoured us by agreeing to evaluate this work.

Finally, we express our sincere thanks to the teaching faculty who helped us directly and indirectly in the completion of this task successfully.

Table of Contents

List of Abbreviations

Abbreviation	Definition
PV	Photo-Voltaic
a-Si	Amorphous Silicon
DC	Direct Current
STC	Standard Test Conditions
NOCT	Nominal Operating Cell Temperature
MPP	Maximum Power Point
FF	Fill Factor
SD	Single Diode
DD	Double Diode
EMF	Electro-Magnetic Force
MPPT	Maximum Power Point Tracking
P&O	Perturb and Observe
IncCond	Incremental Conductance
AI	Artificial Intelligence
DE	Differential Evolution
TLABC	Teaching Learning based Artificial Bee Colony
WCA	Water Cycle Algorithm
PSO	Particle Swarm Optimizer
LMGWO	Levenberg-Marquardt Grey Wolf Optimizer
EA	Evolutionary Algorithm
RMSE	Root Mean Square Error
Rcr-IJADE	Repaired crossover rate improved J.Adaptive Differential Evolution
L-SHADE	Linear Success History Adaptive Differential Evolution
OP	Opposite Population
ABC	Artificial Bee Colony
MCSWOA	Modified Search Strategies Assisted Crossover Whale Optimization Algorithm
IAE	Individual Absolute Error
MAE	Mean Absolute Error
BWO	Black Widow Optimizer

List of Symbols

Symbol	Description	Unit
E	Energy	J
λ	Wavelength	m
h	Planck's constant	J.s
c	Speed of light	m/s
V	Voltage	V
G	Solar irradiance	W/m^2
T	Temperature	K
AM	Air mass	-
P	Power	W
I	Current	A
η	Efficiency	-
A	Area	m^2
pMax	Temperature coefficient	-
R	Resistance	Ω
a	Ideality factor	-
k	Boltzmann’s constant	J/K
q	Electron charge	C
CR	Crossover rate	-
NP	Number of population	-
F	Mutation factor	-
Ns	Number of cells	-
Eg	Energy bandgap Temperature	eV
Ki	Coef. of current	-
PR	Procreating rate	-
MR	Mutation rate	-

List of Figures

List of Tables

General Introduction

Solar energy is becoming the most popular renewable energy used in the world, due to its environmental and economic benefits. In addition, the extensive use of fuels and their negative effect on the environment will at a point force humanity to rely on sustainable energies.

Solar energy has gained great attention from researchers in the last years; their concern is the simulation and forecasting of the behaviour of PV systems under different conditions. The PV is manufactured from a semiconductor material that converts light into electricity. Its performances are affected by many factors, external such as temperature and irradiance, shading, dust, wind velocity; and internal factors related to the design and modelling.

In order to study electronic converters for PV systems, one first needs to know how to model the PV device that is attached to the converter. Hence, it is necessary to find an accurate model and identify its parameters that effectively describe the nonlinear current-voltage characteristic; in order to develop controlling techniques for maximum power point tracking that is based on electronic converters. Hence, optimize the power generated.

The identification of PV model parameters is a complex, multi-variable, highly non-linear, multi-model problem. The challenge is to obtain the values of all parameters while keeping a reasonable compromise of some criteria, such as the fast speed of convergence, accuracy, and robustness.

The report is organized as follow:

- In the first chapter, a theoretical background about photovoltaic systems is presented.
- In the second chapter, opposition-based differential evolution optimization algorithm is used to extract the PV unknown parameters for single and double diode models based on the experimental I-V data and results are compared at the end with other well-known meta-heuristic algorithms.

- In the third chapter, a new method is developed in order to extract the unknown parameters of the single diode model based on manufacturer's data and results are also compared with other methods.
- Finally, we end up with a general conclusion and further work.

Chapter 1

Photovoltaic Systems

1.1 Solar Radiation

The Sun is a hot sphere of gas whose internal temperature reaches over 20 million Kelvin and the temperature at the surface around 6000 Kelvin. The light that we see everyday is only a fraction of the total energy emitted by the sun incident on the Earth. Sunlight is a form of "electromagnetic radiation" and the visible light is a small subset of the electromagnetic spectrum which describes the light as a wave.

Light consists of particles of energy, called photons which are characterized by either a wavelength, denoted by λ or energy, denoted by *E*. There is an inverse relationship between the energy of a photon (*E*) and the wavelength of the light (λ) given by the equation:

$$E = \frac{h.c}{\lambda} \tag{1}$$

Where *h* is Planck's constant (6.626×10^{-34} joule.s) and *c* is the speed of light (2.998×10^{8} m/s). When dealing with photons and electrons, a commonly used unit of energy is the electron-volt (eV) instead of joule (J). An electron volt is the energy required to raise an electron through 1 volt, thus a photon with an energy of 1 eV = 1.602×10^{-19} J.

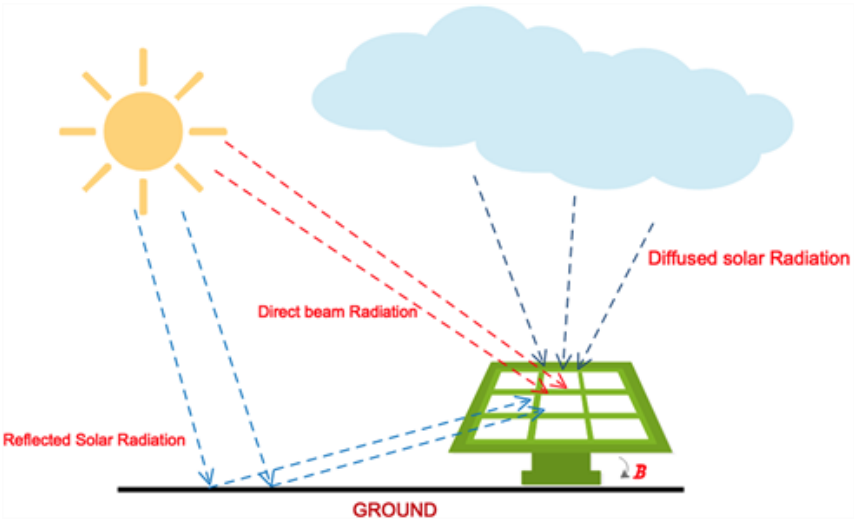

Figure 1.1 *Solar radiation.*

While the solar radiation incident on the Earth's atmosphere is relatively constant, the radiation at the Earth's surface varies widely due to atmospheric effects, latitude of location, and the season of the year and the time of day. The radiation received by a surface has three components: direct, diffuse and reflected radiations.

1.2 Photovoltaic cells

The first conventional photovoltaic cells were produced in the late 1950s and were deployed to provide power for satellites. A solar cell is a solid-state semiconductor p-n junction device that converts light into Direct-Current electricity through the principle of photovoltaic effect.

1.2.1 Principle of working and construction

The starting point for most generations of PV devices is Crystalline Silicon which is referred to Group IV of the periodic table. At absolute zero temperature, Silicon is a perfect insulator. As it gets warmer, some electrons will be given enough energy to free from their nuclei and hole-electron pairs will be created, which results in electricity flow. A photon with more than 1.12eV which is the energy gap of Silicon and a wavelength less than 1.11 μm; will make a single electron jump to the conduction band. To avoid recombination, a p-n junction is created by adding impurities (doping) into silicon, the n-region is doped with phosphorus-atoms and it is a thick layer, whereas the p-region with boron atoms and is thinner. This will create a built-in electric field in the semiconductor itself that pushes electrons in one direction and holes in the other.

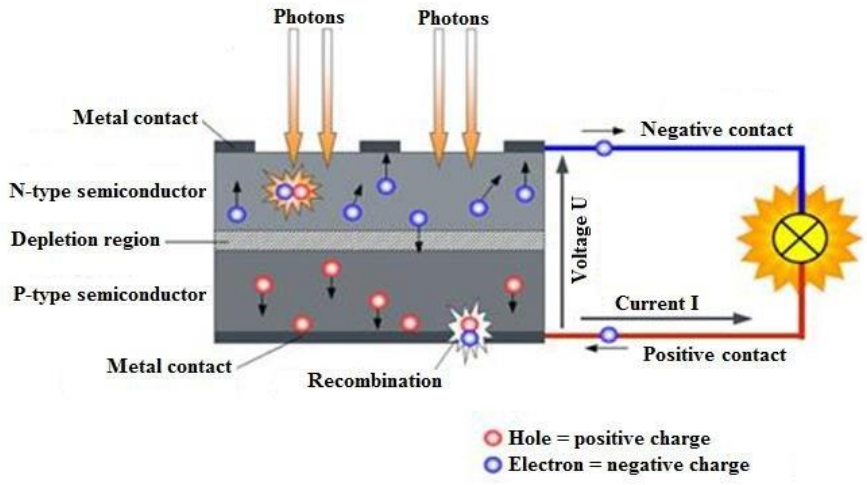

Figure 1.2 *Solar cell structure and working principle.*

The electrical contact on the top surface of the cell presents in some grid pattern and is composed of a good conductor such as metal. Since metal blocks light, the grid lines are thin and widely spaced. The back electrical contact layer has no such restrictions. It simply functions as an electrical contact and thus covers the entire back surface of the cell and it is also made of metal. The solar cell is covered by a thin glass to protect it from any mechanical shock.

1.2.2 Photovoltaic types

There are three types of PV cell technologies: monocrystalline silicon, polycrystalline silicon, and thin film. There are other technologies such as gallium arsenide but they are less common due to their high cost.

- **Monocrystalline silicon cell:** the first commercially available cell, it is an extremely pure form of silicon, it contains a single uniform crystal structure, with high efficiency (15%); however, they are expensive comparing to the other two technologies due to their manufacturing complexity.
- **Polycrystalline silicon cell:** it contains many small grains of crystals instead of a single uniform crystal structure; they dominate the world market, representing about 70% of global PV production in 2015 [1]. Its efficiency is around 12%.
- **Thin film cell:** cells can also be made from a thin film which makes them more flexible and durable. A common type of thin film PV cell is amorphous silicon (a-Si). It is produced by depositing thin layers of silicon onto a glass substrate. It uses less than 1% of the silicon needed for a crystalline cell which makes it cheaper but its efficiency is reduced (6%).

1.2.3 Photovoltaic configurations

A typical silicon PV cell produces about 0.5 – 0.6 V DC under open-circuit and no-load conditions, which is very small. Hence, Solar cells can be arranged into large groupings. They are connected in series and/or parallel circuits to produce higher currents, voltages, and power levels. PV modules consist of PV cells sealed in a laminate. PV panels include one or more PV modules assembled as pre-wired, field-installable units. The back of each solar panel is equipped with standardized sockets so that its output can be combined with other solar panels to form a solar array.

Photovoltaic systems are classified as either stand-alone or grid-connected systems. Stand-alone systems contain a solar array and a bank of batteries directly wired to an application or load circuit. Grid-connected systems integrate solar arrays with public utility power grids in two ways. One-way systems are used by utilities to supplement power grids during peak usage. And bidirectional systems are used by companies and individuals to supply their power needs, with any excess power fed back into the utility power grid.

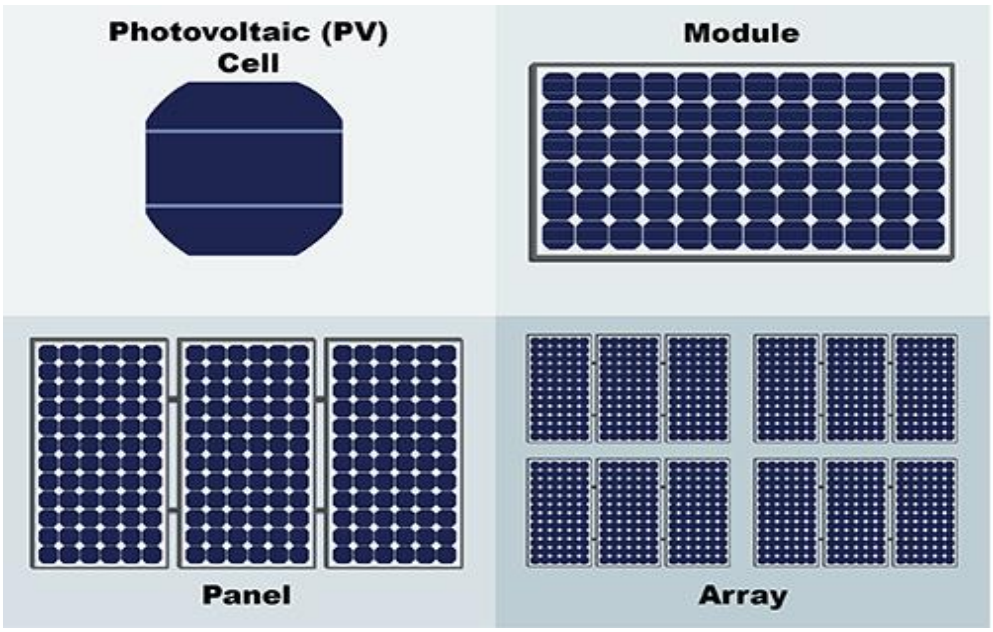

Figure 2.3 *Photovoltaic Configurations.*

1.2.4 Standard Test Conditions:

The parameters provided in datasheets by manufacturers are under Standard Test Conditions (STC), which allow us to compare between different panels.

These conditions are specified as follows:

- Solar irradiance of 1000 W/m^2.
- Cell temperature of 25^{0}C.
- Air mass of AM =1.5

In addition, Nominal Operating Cell Temperature is provided, which is the cell temperature in a module when ambient temperature is 20°C, solar irradiance is 8000 W/m^2, and wind speed is 1 m/s. To account for other ambient conditions, the following expression may be used:

$$Tcell = Tamb + \left(\frac{NOCT - 20^{\circ}}{0.8}\right) G \qquad (2)$$

Where Tcell is the cell temperature (°C), Tamb is the ambient temperature (°C) and G is the solar irradiance (kW/m^2).

1.3 Performance of photovoltaic cells

1.3.1 Electrical Characteristics

Solar Cell I-V and P-V Characteristic Curves show the current, voltage, and power characteristics of a particular PV cell, module, or array. Knowing these characteristics (more importantly Pmax) of a panel is critical in determining its output performance and solar efficiency. These curves provide the information required to configure solar systems. The I-V curve of a cell or a module is generally provided by manufacturers as well as its datasheet under standard test conditions (STC).

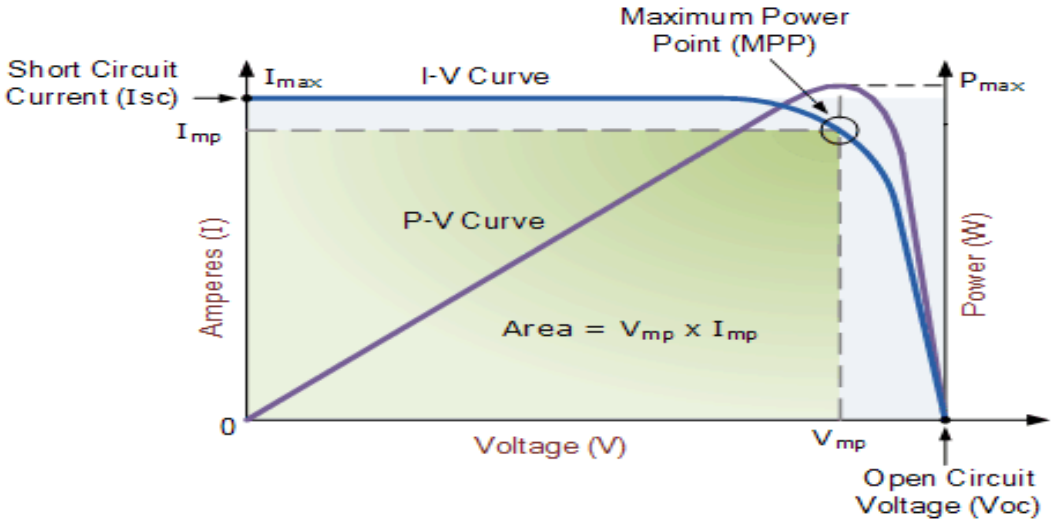

Figure 1.4 *I-V and P-V characteristic curves.*

The MPP can be located by finding the biggest possible rectangle that will fit inside the I-V curve. To this, a factor that quantifies the maximum power of the module is the fill factor (FF). The higher is the fill factor, the greater is the efficiency of the PV cell.

$$FF = \frac{Power\ at\ mpp}{Theoritical\ maximum\ power} = \frac{Vmp.Imp}{Voc.Ish} \quad (3)$$

Every solar panel has multiple I-V curves, one each for all the different combinations of conditions that would affect the STC ratings. The ideal position on any I-V curve where we can collect the most power from the module is at the “knee”. That’s the maximum power point (MPP), and its position changes with temperature and irradiance. Solar irradiance controls the amount of output current, and the operating temperature affects the output voltage.

In order to model PV cells we need three important points which are the ones given in datasheets by manufactures, these points are:

- **Open-Circuit Voltage:** This is the maximum voltage that the cell provides when the terminals are not connected to any load (open circuit condition).
- **Short-Circuit Current:** This is the maximum current provided by the cell when the terminals are shorted (short circuit condition).
- **Maximum power point:** This is the point where the power supplied by the cell that is connected to the load (batteries, inverters) is at its maximum value, where Pm = Im x Vm.

1.3.2 Photovoltaic efficiency

Solar cell efficiency refers to the ratio of the power output of a solar cell to its power input while considering its surface area. It is the portion of energy in the form of sunlight that can be converted via photovoltaic into electricity by the solar cell. It can be calculated as follows:

$$\eta = \frac{Pmax}{A.G} \times 100\ \% \quad (4)$$

Where Pmax is the maximum power (W), A is the area of the panel (m^2) and G is the irradiance at STC (1000 W/m^2).

1.4 Temperature and irradiance effects

Like all semiconductors, increase in temperature reduces the bandgap of the semiconductor. Hence, increasing the energy of electrons in the material, so less energy is required to break the bonds and the potential difference is decreased. The open circuit voltage is the most affected by the temperature. In the other hand, the short circuit current is the most affected by the light intensity; as it increases, the current increases.

If we look at the datasheet provided by manufactures, a term called temperature coefficient (pMax) is usually presented. It is given in percentage and reveals the impact of temperature on the panel. Panels are usually tested at 25^0C, if the coefficient is for example -0.20%, then for every 1^0C rise, the maximum power drops by 0.20%. Each type of solar cell has a different temperature coefficient.

- Monocrystalline and polycrystalline cells: -0.45% to -0.50%.
- Amorphous based thin film panels: -0.20% to -0.25%.

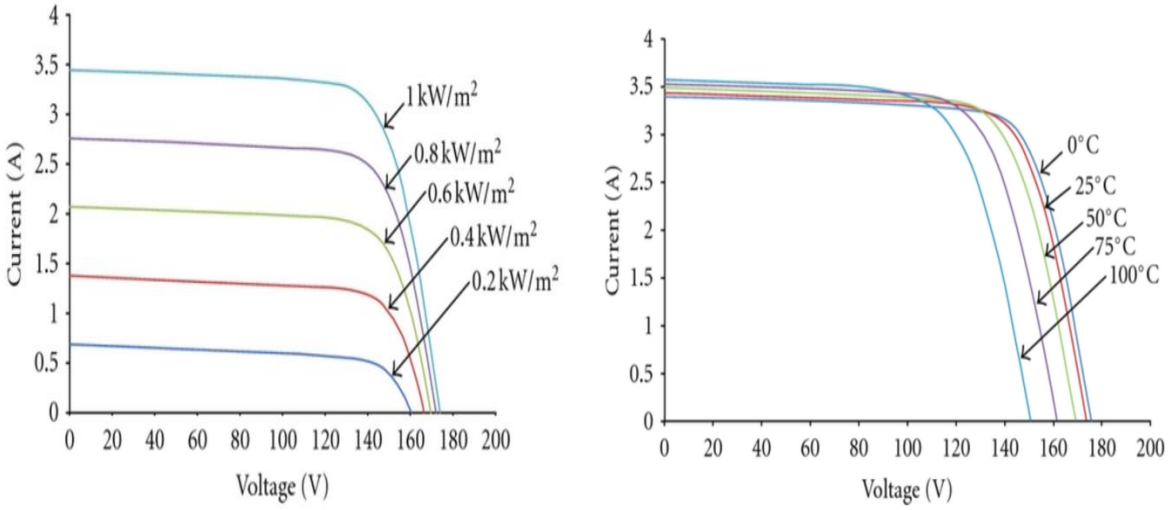

Figure 1.5 *Effect of temperature and irradiance.*

1.5 Mathematical Model of PV cell

There are several electrical models, used by researchers, to describe the physical behaviours of PV cells. The two common models are single diode (SD) and double diode (DD) models.

1.5.1 Single Diode Model:

The single diode model is the traditional PV model known as the five parameters model; it provides a good compromise between accuracy and simplicity.

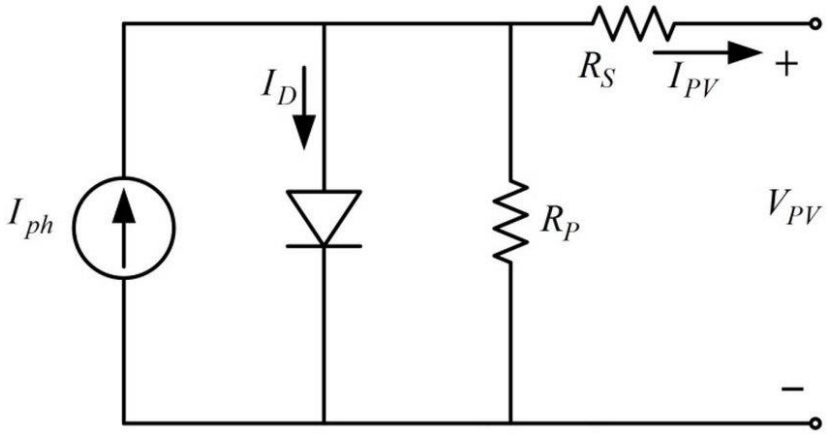

Figure 1.6 *Single diode model.*

It consists of a diode in parallel with a current source and two resistors; the diode represents the p-n junction while the current source represents the current induced by the cell. The parallel resistor accounts for leakage current, and the series resistor represents losses related to load current. Therefore, the output current of the single diode model can be calculated as follows:

$$I = Iph - Id - Ip \tag{5}$$

Where I denotes the output current, Iph represents the photo-generated current, Id is the diode current, and Ip is the current through the parallel resistor.

Considering the Shockley equation, the diode current is written as Eq. (6), while the current Ip is formulated as Eq. (7).

$$Id = Is\left(e^{\frac{V+Rs.I}{a.Vt}} - 1\right) \tag{6}$$

$$Ip = \frac{V+Rs.I}{Rp} \tag{7}$$

Where Is is the reverse saturation current of the diode. V denotes the terminal voltage, Rs and Rp series and parallel resistors respectively, a is the diode ideality factor. Vt is the junction thermal voltage and is defined by Eq. (8).

$$V_t = \frac{T.K}{q} \tag{8}$$

Where T indicates the cell temperature in Kelvin, k is the Boltzmann constant (1.381×10^{-23} J/k), and q is the electron charge (1.602×10^{-19}C). Based on the equations above, the final equation representing the single diode model is formulated as Eq. (9).

$$I = I_{ph} - I_S\left(e^{\frac{V+Rs.I}{a.Vt}} - 1\right) - \frac{V+Rs.I}{Rp} \tag{9}$$

1.5.2 Double Diode Model:

In the single diode model, the equation assumes that the ideality factor is constant. In fact, it is a function of voltage across the cell; at high voltage, the recombination is dominated by the surfaces and the ideality factor is close to one. However at low voltage, recombination in the junction dominates and the ideality factor is close to two. So, taking in consideration the

effect of recombination in the depletion region, the double diode model is developed. It is reported to have better accuracy. And it is known as the 7-parameters model.

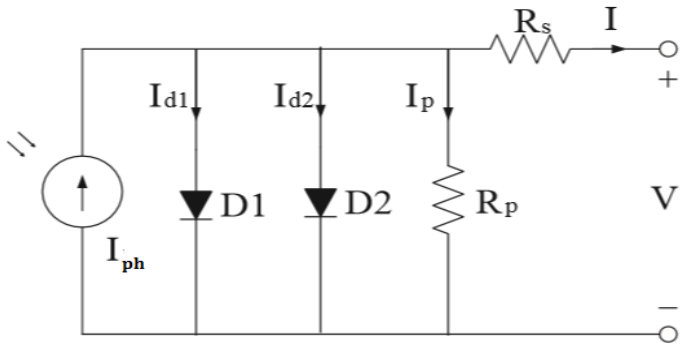

Figure 1.7 *Double diode model.*

With the same analogy as the single diode model, the equation representing the double diode model is defined in Eq. (10).

$$I = I_{ph} - I_{s1}\left(e^{\frac{V+I.R_S}{a1.Vt}} - 1\right) - I_{s2}\left(e^{\frac{V+I.R_S}{a2.Vt}} - 1\right) - \frac{V+I.R_s}{R_p} \qquad (10)$$

1.6 Power losses in solar energy

The maximum efficiency of solar radiation energy can be estimated based on fundamental concepts of thermodynamics; according to Planck's law, it is expressed as follows:

$$\eta = 1 - \frac{4}{3}\frac{To}{Ts} + \frac{1}{3}\left(\frac{To}{Ts}\right)^4 \qquad (11)$$

Where To and Ts are the ambient temperature and the equilibrium temperature of the radiating surface of the sun in Kelvin respectively. For To = 300K and Ts = 5800K, we obtain η =0.93. Unfortunately, this high efficiency is not feasible because of the optical and electrical losses.

1. **Top surface contact obstruction (3%):** the top surface area covers a part of the active surface of the cell.
2. **Reflection at top surface (1%):** anti-reflection coatings can be used on the top surface of the cell to minimize these losses.
3. **Lost photon energy (53.2%):** photon energy less or more than the bandgap will not generate hole-electron pairs and appears as heat.

4. **Voltage factor (20%):** only a part of the potential difference produced for the EMF of an external circuit.
5. **Curve factor (4%):** due to the exponential characteristic, the maximum power is less than (VocIsh) product.
6. **Series resistance (0.3%):** due to the movement of current through the emitter and base of the solar cell, the contact resistance between the metal contact and the silicon; and finally the resistance of the top and rear metal contacts.
7. **Shunt Resistance (0.1%):** it is caused by structural defects across and at the edge of the cell.

1.7 Effect of series and parallel resistances

1.7.1 Series resistance:

Series resistance does not affect the solar cell at open-circuit voltage since the overall current through the series resistance is zero. However, near the open-circuit voltage, the I-V curve is strongly affected by the series resistance. A straight-forward method of estimating the series resistance from a solar cell is to find the slope of the I-V curve at the open-circuit voltage point.

1.7.2 Shunt resistance:

Low shunt resistance causes power losses in solar cells by providing an alternate current path for the light-generated current which reduces the voltage from the solar cell.

The effect of a shunt resistance is severe at low light levels, since there will be less light-generated current. In addition, at lower voltages where the effective resistance of the solar cell is high, the impact of a resistance in parallel is large. The shunt resistance is found using the slope of the I-V curve at the short circuit current point.

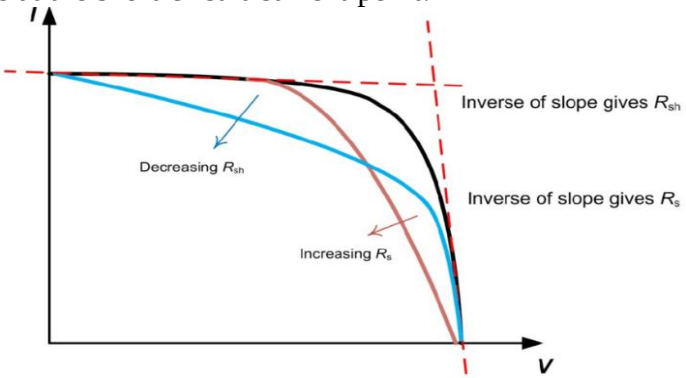

Figure 2.8 *Effect of series and shunt resistances.*

1.8 Maximum Power Point Tracking (MPPT)

The major principle of MPPT is to extract the maximum available power from PV module by making them operate at the most efficient voltage (maximum power point). MPPT checks output of PV module, compares it to battery voltage then fixes what is the best power that PV module can produce to charge the battery. A MPPT solar charge controller is the charge controller embedded with MPPT algorithm to maximize the amount of current going into the battery from PV module.

Among all the algorithms, Perturb and Observe (P&O) and Incremental Conductance (IncCond) algorithms are most common as they have the advantage of an easy implementation.

- **Perturb and Observe:** In this technique, a minor perturbation is introduced to cause the power variation of the PV module. The PV output power is periodically measured and compared with the previous power. The voltage is increased or decreased to check whether the power is increased or decreased. When an increase in voltage leads to an increase in power, this means the operating point of the PV module is on the left of the MPP. Hence further perturbation is required towards the right to reach MPP, if the power decreases when we increase the voltage, the operating point is in the right of MPP.
- **Incremental Conductance:** This algorithm uses the instantaneous conductance I/V and the incremental conductance dI/dV for MPPT. Depending on the relationship between the two values, the location of the operating point of the PV module in the P–V curve can be determined.

1.9 Identification of PV parameters

The process of identification of the PV parameters consists of finding the values of 5 parameters for single diode model, and 7 parameters for double diode model, these parameters are the one presented earlier in Eqs. (9-10). Those equations are highly non-linear (double non linearity, first is due to the exponential itself and second is due to the structure of Rs and a which are in the exponential). These parameters are:

- Diode saturation Current Is.
- Photo-Generated Current Iph.

- ❖ Diode ideality factor a.
- ❖ Series resistance Rs.
- ❖ Parallel resistance Rp.

There is a large volume of literature on identification of PV parameters. However, the methods varied from one research to another. Techniques used for this purpose can be classified into two categories:

1.9.1 Conventional methods:

They depend on the gradient. They identify the parameters mathematically based on some approximations and initial values. [2-4]

Some common techniques are:

- **Gauss Seidal:** it is an iterative method, where the unknowns are expressed in the following form $\boldsymbol{x^{t+1} = f(x^t)}$ and then solved based on initial estimations. The usage of this technique is described in [5].
- **Newton Raphson:** another method for solving non linear equations and it is done by computing the Jacobian linearization of the function around an initial guess point, and using this linearization to move closer to the nearest solutions. The usage of this technique for obtaining the parameters of PV model is described in [6].

1.9.2 Intelligent techniques:

These techniques are meta-heuristic optimization-based methods, using Artificial Intelligence (AI) inspired algorithms. They use bio-inspired algorithms in the search process to identify the PV parameters values at real-time. The main reason behind the success of these algorithms is that they use commonly shared information among multiple agents. They are classified into three categories: evolutionary algorithms, swarm-intelligence based algorithms and physical phenomenon based algorithms.

- **Evolutionary algorithms:** like genetic algorithms, evolution strategies, differential evolution (DE) [7], etc) mimic various aspects of evolution in nature such as survival of the fittest, reproduction and genetic mutation.

- **Swarm-intelligence algorithms:** mimic the group behaviour and/or interactions of living organisms (like ants, bees (teaching learning based artificial bee colony (TLABC) [8]), birds, spiders, white-blood cells, bacteria, etc.) and non-living things (like water (WCA) [9], river systems, masses under gravity, etc.). One common method is particle swarm optimization (PSO) [10].
- The rest of the meta-heuristics mimic various physical phenomena like annealing of metals, musical aesthetics (harmony), etc

➢ Hybrid techniques also exist; they are a combination of conventional methods and intelligent optimization techniques such as hybrid Levenberg-Marquardt - grey wolf optimizer (LMGWO) [11].

1.10 Disadvantages of solar energy

In a single hour, the amount of power that the earth receives from the sun is more than the entire world's consumption in a year. We have a source of virtually unlimited clean energy that is wasted on the surface. However, we still using so little of it; since batteries that can store such an amount of energy are not developed yet, the other issue is the ability to capture all this energy, a typical array used in houses can only convert 14% of the energy it captures. While the ones developed in laboratories can exceed 30%. In addition, its high installation cost, and the fact that solar panels are dependent on sunlight to effectively gather solar energy. Therefore, a few cloudy, rainy days can have a noticeable effect on the energy system.

1.11 Conclusion

Since, solar energy has proven to be a competent energy resource; due to its huge potential and inexhaustible nature. The challenge now is to make considerable improvements in order to overcome its disadvantages mentioned previously. In this chapter, we discussed some background knowledge on photovoltaic materials and solar energy principles required to understand future parts of this report. Photovoltaic parameters and models were presented as well as solar energy efficiency and factors affecting it. We also presented a brief definition of the MPPT which allows maximum power extraction. Two important models are the single and double diode models which as we saw have highly non-linear characteristics that make it

hard to find the PV parameters. Therefore, several techniques and algorithms were developed to make the process easier and more accurate.

In the following chapters, we will test and simulate two techniques to identify the parameters of photovoltaic cells/Modules based on the experimental current-voltage data and the datasheet provided by manufacturers.

Chapter 2

Identification of PV parameters using Opposition-based DE

2.1 Introduction

Optimization has been a topic of great interest in recent years, and meta-heuristic search methods proved to be very efficient for handling difficult optimization problems that are large, complex, non-linear and multimodal.

One of the common types of optimization algorithms is evolutionary algorithms (EA) which are a simulation of the biological evolution process; they are useful for any optimization problem, particularly when conventional calculus-based optimization techniques fail to solve difficult problems. EAs can always reach the near-optimum or the global maximum. Furthermore, they tend to be versatile and stable.

In this section, Differential Evolution algorithm (DE) based on opposite population is proposed in order to identify the parameters of the PV model. In the parameter estimation problem, the main objective is to minimize the difference between the measured and simulated current data. Experimental results are presented at the end to prove the efficacy of the proposed approach.

2.2 Objective Function

In order to use any optimization technique, the primary task is to define the fitness function or the objective function of the problem that needs to be minimized. To quantify the error between the measured and simulated data, the root-mean-square error (RMSE) is used. First, the current error functions for single and double diode models are defined as follows:

- For the single Diode model for a PV module of Ns cell:

$$\begin{cases} F(V,I,X) = I_{ph} - I_s\left(e^{\frac{V+R_s.I}{Ns.a.V_t}} - 1\right) - \dfrac{V+R_s.I}{R_p} - I \\ X = \{a, R_s, R_p, I_{ph}, I_s\} \end{cases} \quad (12)$$

- For the double diode model:

$$\begin{cases} F(V,I,X) = I_{ph} - I_{s1}\left(e^{\frac{V+I.R_s}{Ns.a_1.V_t}} - 1\right) - I_{s2}\left(e^{\frac{V+I.R_s}{Ns.a_2.V_t}} - 1\right) - \dfrac{V+I.R_s}{R_p} - I \\ X = \{a_1, a_2, R_s, R_p, I_{ph}, I_{s1}, I_{s2}\} \end{cases} \quad (13)$$

Then, the RMSE is defined as the objective function and it is formulated by Eq. (14) where N is the number of measured data.

$$f = RMSE = \sqrt{\frac{1}{N}\sum_{k=1}^{N} F(V,I,X)^2} \quad (14)$$

As we can see the problem of estimating the PV parameters is formulated as an optimization problem where the fitness function must be minimized by searching the optimal vector X.

2.3 Differential Evolution

Differential evolution is one of the popular evolutionary algorithms. It was originally proposed by Storn and Price in 1995 [12]. It is a population-based meta-heuristic search method that optimizes a problem by improving a candidate solution iteratively based on several evolution stages. Such techniques need few or no assumptions on the problem since they can explore very large spaces. The algorithm searches the problem space by maintaining the candidate solution and creating new solutions by combining existing ones. The solutions with the best objective functions are kept for next iterations till reaching an optimum solution.

DE starts with an initial random population vector that contains NP D-dimensional candidate individuals. The individuals of the G^{th} iteration can be represented by $P^G = (X_1^G, X_2^G ... X_{NP}^G)$ where $G = 0, 1 ... G_{max}$ denotes the number of iteration. Each candidate individual is a D-dimensional target vector that can be represented by $X_i^G = (x_{i,1}, x_{i,2} ... x_{i,D})$ where i denotes the i^{th} individual that has D parameters.

For our specific problem, the parameters to be optimized are 5 parameters for the single diode model and 7 parameters for the double diode. The population vector of the G^{th} iteration for the single diode case can be represented as follows:

$$P^G = \begin{Bmatrix} a^i & \dots & a^{NP} \\ Rs^i & \dots & Rs^{NP} \\ Rp^i & & Rp^{NP} \\ Iph^i & & Iph^{NP} \\ Is^i & & Is^{NP} \end{Bmatrix} \text{ D parameters} \quad (15)$$

NP individuals

Then, the individuals enter a loop of three stages of the evolutionary process. The step-by-step procedure is as follows:

- **Initialization:** the initial population of the i^{th} individual is randomly generated within a predefined bound as follows:

$$X_{i,j} = L_j + (H_j - L_j) \times rand(0, 1) \qquad j = 1, 2 \ldots D \tag{16}$$

Where rand (0, 1) returns a single uniformly distributed random number in the interval (0, 1), L_j and H_j and the lower and upper in the j^{th} dimension, respectively.

- **Mutation:** the standard mutation operator of DE needs three randomly selected different individuals from the current population for each individual to form the mutant vector V_i. It prevents premature local convergence and ensures global convergence in the final stage. A frequently used mutation strategy denoted DE/rand/1 where the mutated individual is generated for each individual X_i^G as follows:

$$V_i^G = X_{r1}^G + F \times (X_{r2}^G - X_{r3}^G) \qquad i = 1, 2 \ldots NP \tag{17}$$

The subscripts r1, r2, r3 are distinct randomly generated integers selected from 1 to NP that are unequal to the index i. F is the mutation scaling factor that controls the amplification of the mutation ($F \in (0, 1)$).

- **Crossover:** to increase the diversity of the population, the mutated individual V_i^G is mated with X_i^G, generating the trial vector U_i^G. The genes of this vector are inherited from X_i^G and V_i^G.

$$U_{i,j}^G = \begin{cases} Vi,j^G & \text{if } randi,j(0,1) \leq CR \\ Xi,j^G & \text{if } randi,j(0,1) > CR \end{cases} \tag{18}$$

Where $rand_{i,j}$ (0, 1) is a random number between 0 and 1, CR represents the crossover rate that controls the crossover process ($CR \in (0, 1)$).

- **Selection:** in this final stage, the DE uses the objective functions to decide whether the trial vector or the target vector is kept for next iteration. Where f(x) is the objective function or the fitness function to be minimized.

$$X_i^{G+1} = \begin{cases} Ui^G & \text{if } f(Ui^G) \leq f(Xi^G) \\ Xi^G & \text{if } f(Ui^G) > f(Xi^G) \end{cases} \tag{19}$$

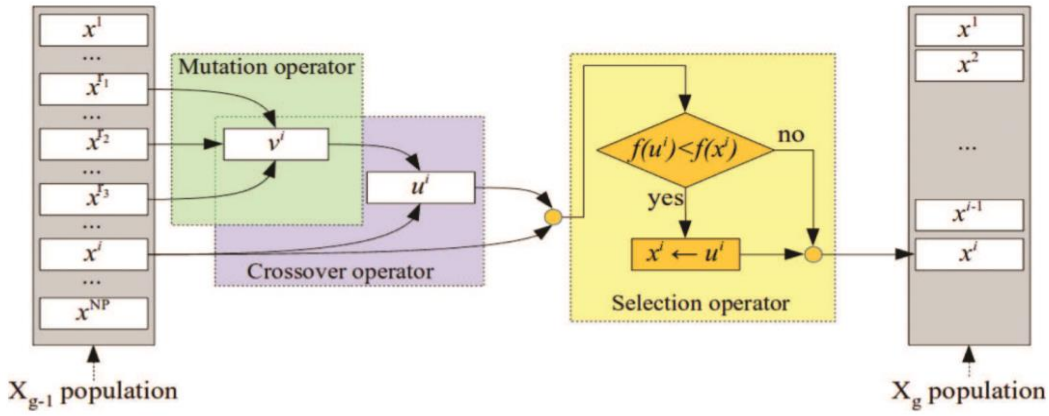

Figure 2.1 *Evolutionary process of DE algorithm* [13].

- Although the classical DE is simple, efficient and has only three parameters to be controlled, researchers have tried to enhance its performance by creating DE variants such as Rcr-IJADE and L-SHADE that proved to have better accuracy in solving complex problems.
- In our proposed algorithm and in order to identify the parameters of the PV model, DE is enhanced in terms of accuracy and speed using opposition-based population proposed in [14].

2.4 Opposition-based Learning

The main idea behind the opposition-based learning is considering the estimate and opposite estimate or in other term guess and opposite guess at the same time in order to achieve a better approximation for current candidate solution. This idea is suitable for all evolutionary algorithms and can be used for a wide range of optimization problems.

As previously mentioned, DE starts with some initial population; this estimation is considered a random guess. We can improve our chance to start with a closer guess by checking the opposite solution simultaneously. In fact, according to probability theory, in 50% of cases, the guess is farther from the solution than the opposite guess; and that can accelerate convergence and enhance accuracy [14].

2.4.1 Definition

First we should define the opposite number or point, let P (x_1, x_2 ... x_n) be a point in n-dimensional space where $x_i \in [ai, bi]$ i = (1, 2 ... n). The unique opposite point of P is defined by $\tilde{P}(\tilde{x}_1, \tilde{x}_2 \dots \tilde{x}_n)$ where:

$$\tilde{x}_i = a_i + b_i - x_i \quad (20)$$

2.4.2 Opposition-based optimization

Let the point P(x_1, x_2 ... x_n) be a candidate solution or population and f (x) is the fitness function used for the optimization problem, according to the opposite point principle, the point $\tilde{P}(\tilde{x}_1, \tilde{x}_2 \dots \tilde{x}_n)$ is the opposite population of P; if f ($\tilde{P}$) ≤ f (P), the solution P should be replaced by $\tilde{P}$, otherwise P is kept. So, the procedure is applied to the DE algorithm as follows:

(1) Generate a random population P of size NP.

(2) Calculate the opposite population OP of size NP according to the following equation:

$$OP_{i,j} = a_j + b_j - P_{i,j} \quad i = 1, 2 \ldots NP \quad \text{and} \quad j = 1, 2 \ldots D \tag{21}$$

(3) Compare population and opposite population using the fitness function and select the fittest.

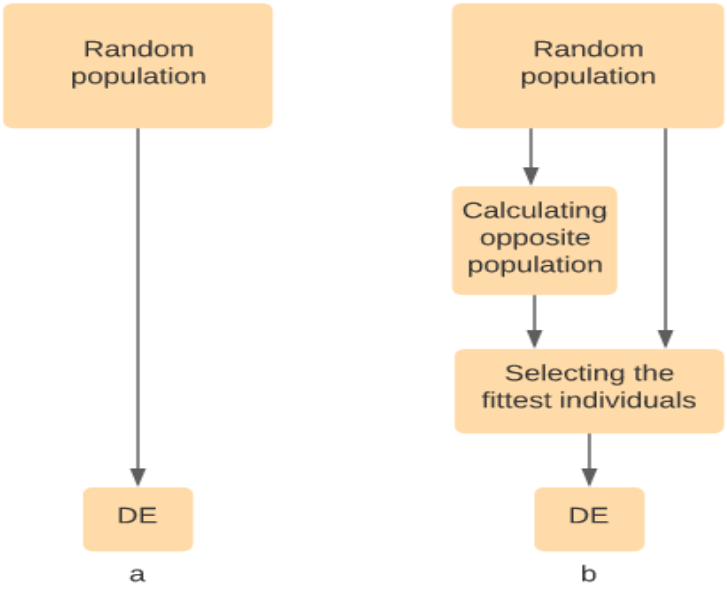

Figure 2.2 *DE with (a) classical random population initialization and (b) opposition-based population.*

2.5 Proposed Algorithm

By adding the opposition-based population into the DE algorithm, the proposed algorithm is developed and presented in Algorithm 1. Compared to original DE, it can be seen that it needs only a small extra computational cost in calculating the opposite population and comparing the fitness values. The structure remains simple and no new parameter to be adjusted. The process of identifying the parameters of the PV model using the proposed algorithm is presented in the following flowchart.

Algorithm 1: The main procedure of the proposed DE

Input: Control parameters CR, NP, F.

Output: Optimal solution.

1 **Initialization**: Generate random population P of NP individuals of D dimension using Eq. (16).

2 Calculate opposite population OP using Eq. (21).

3 Calculate the fitness values of both P and OP using Eq. (14).

4 Select the fittest individuals to create the new population.

5 For G = 1 to Gmax do

6 For i = 1 to NP do

7 **Mutation**: Generate mutated vector using Eq. (17).

8 **Crossover**: Generate trial vector using Eq. (18).

9 **Selection**: Select the fittest individuals for next iteration using Eq. (19).

10 End For

11 End For

12 End procedure

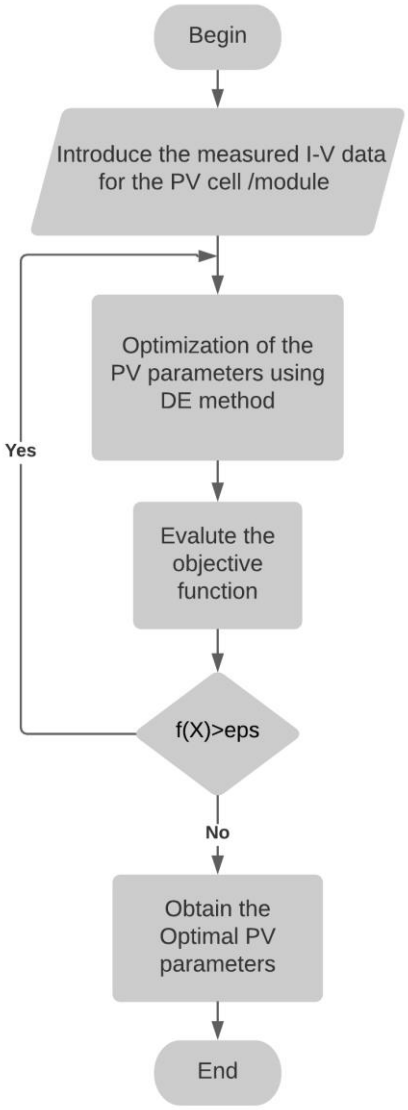

Figure 2.3 *Flowchart of the PV parameters identification process.*

2.6 Results and Discussion

In this section, the proposed DE algorithm is applied to extract the parameters of two different models; the single diode and double diode models. In order to have a fair comparison with other algorithms, we used the 57mm diameter commercial R.T.C France silicon cell, the Photowatt-PWP-201, STP6-120/36 and STM6-40/36 modules. Furthermore, the algorithm is tested on other different PV modules to prove its effectiveness.

The algorithm is implemented in MATLAB R2016a and all simulations are executed on a PC with Intel(R) Celeron(R) N3050 processor @ 1.60GHz 1.60GHz, 4GB RAM, under the Windows 8 64-bit OS.

The experimental I-V data used are the ones in [15]. The electrical specifications of the cell and modules as well as the temperature values are presented in Table 1.

Table 1 Electrical specification of the PV cell/modules.

Parameter	RTC France	Photowatt-PWP-201	STP6-120/36	STM6-40/36
Type	Poly-crystalline	Poly-crystalline	Poly-crystalline	Mono-crystalline
Vm (V)	0.4507	12.6490	14.9300	16.9800
Im (A)	0.6880	0.9120	6.8300	1.5000
Voc (V)	0.5728	19.7780	19.2100	21.0200
Ish (A)	0.7603	1.0300	7.4800	1.6630
Ns	1	36	36	36
Temperature (°C)	30	45	55	51

- **Experimental Settings:**

  In this work, the maximum number of iterations is 500 for single diode and 1000 for double diode. With regard to other parameters associated with the compared algorithms, the same values in their original literature were used for a fair comparison. The parameter settings for the algorithms are presented in Table 2.

Table 2 Parameter settings of the opposition-based DE and the compared algorithms.

Algorithm	Parameter Setting
Proposed DE	NP = 50, CR = 0.9, F = 0.5
DE [7]	NP = 50, CR = 0.9, F = 0.5
Rcr-IJADE [7]	NP = 50, F = 0.5
ABC [16]	NP = 50
MCSWOA [17]	NP = 50
LMGWO [11]	-
TLABC [8]	NP = 50, limit = 200, F = rand (0,1)

The search ranges used are the ones proposed in [18] which proved to lead to a better accuracy than other proposed ranges. These constraints are:

$$1 \leq a_1 and\ a_2 \leq 2 \quad (22.a)$$

$$0 \leq I_{s1} and\ I_{s2} \leq 5\ \mu A\ or\ 1 \mu A \quad (22.b)$$

$$0.95Ish \leq I_{ph} \leq 1.05Ish \quad (22.c)$$

$$0 \leq R_s \leq \frac{Voc-Vm}{Im} \quad (22.d)$$

$$\frac{Vm}{Ish-Im} \leq R_p \leq 100\ or\ 2000 \quad (22.e)$$

Case study #1: R.T.C France Solar cell

The extracted values for the RTC France solar cell for the single diode and the double diode models with the RMSE values are presented in Tables 3 and 4. These values are also compared with those obtained by the other selected algorithms. Comparisons illustrate that the RMSE values of the proposed DE (8.2452×10^{-4} for single diode and 7.9774×10^{-4} for double diode model) are better than the original DE. It indicates that the opposition-based principle increased the performance of the DE. In addition, it outperformed all other algorithms which are DE [7], Rcr-IJADE [7], ABC [16], MCSWOA [17] and TLABC [8]. We can see that the proposed algorithm Opposition-based DE can be used as an efficient and reliable alternative method for parameter identification problems in different PV models.

Table 3 Model parameters for the single diode model, achieved by different optimisation algorithms.

Algorithm	I_{ph}(A)	I_s(μA)	R_s(Ω)	R_p(Ω)	a	RMSE
Proposed DE	0.7608	0.3165	0.0364	53.6271	1.4791	**8.2452e-04**
DE [7]	0.7608	0.3230	0.0364	53.7185	1.4812	9.8602e-04
Rcr-IJADE [7]	0.7608	0.3230	0.0364	53.7185	1.4812	9.8602e-04
ABC [16]	0.7610	0.3348	0.0359	48.7845	1.4830	8.8636e-04
MCSWOA [17]	0.7608	0.3230	0.0364	53.7185	1.4812	9.8602e-04
TLABC [8]	0.7607	0.3230	0.0363	53.7163	1.4811	9.86022e−04
LMGWO [11]	0.7607	0.3230	0.0337	53.7222	1.4811	9.8601e-04

Table 4 Model parameters for the double diode model, achieved by different optimisation algorithms.

Algorithm	I_{ph}(A)	I_{s1}(μA)	I_{S2}(μA)	R_s(Ω)	R_p(Ω)	a_1	a_2	RMSE
Proposed DE	0.7608	0.9907	0.1701	0.0373	55.0644	1.9741	1.4267	**7.9774e-04**
DE [7]	0.7608	0.3756	0.2715	0.0366	54.5704	1.9999	1.4664	9.8344e-04
Rcr-IJADE [7]	0.7608	0.7493	0.2260	0.0367	55.4854	2.0000	1.4510	9.8248e-04
ABC [16]	0.7607	0.2886	0.2474	0.0366	58.2995	1.9683	1.4691	8.0824e-04
MCSWOA [17]	0.7608	0.7974	0.2206	0.0368	53.6255	2.0000	1.4490	9.8602e-04
TLABC [8]	0.7608	0.4239	0.2401	0.03667	54.6679	1.9075	1.4567	9.8414e−04

To further confirm the quality of the results, using these extracted parameters the output current could be easily calculated and given in Tables 5 and 6. Two error metrics, i.e., individual absolute error (IAE) and the mean absolute error (MAE) were used to evaluate the fitting results between the calculated current and the measured current. We can see that for the single diode model the mean absolute error is 0.071 % and for double diode 0.068 %, it means that the calculated values are highly in coincidence with the measured data over the whole voltage range.

Table 5 The calculated current and absolute error results for SD model.

Item	V (V)	I (A)	I calculated (A)	IAE
1	-0.2057	0.7640	0.7642	0.0002
2	-0.1291	0.7620	0.7627	0.0007
3	-0.0580	0.7605	0.7614	0.0009
4	0.00057	0.7605	0.7602	0.0003
5	0.0646	0.7600	0.7590	0.0010
6	0.1185	0.7590	0.7580	0.0010
7	0.1678	0.7570	0.7570	0.0000
8	0.2132	0.7570	0.7560	0.0010
9	0.2545	0.7555	0.7550	0.0005
10	0.2924	0.7540	0.7536	0.0004
11	0.3269	0.7505	0.7513	0.0008
12	0.3585	0.7465	0.7473	0.0008
13	0.3873	0.7385	0.7401	0.0016
14	0.4137	0.7280	0.7275	0.0005
15	0.4373	0.7065	0.7072	0.0007
16	0.4590	0.6755	0.6756	0.0001
17	0.4787	0.6320	0.6304	0.0016
18	0.4960	0.5730	0.5724	0.0006
19	0.5119	0.4990	0.4997	0.0007
20	0.5265	0.4130	0.4136	0.0006
21	0.5398	0.3165	0.3172	0.0007
22	0.5521	0.2120	0.2120	0.0000
23	0.5633	0.1035	0.1026	0.0009
24	0.5736	-0.0100	-0.0093	0.0007
25	0.5833	-0.1230	-0.1244	0.0014
26	0.5900	-0.2100	-0.2091	0.0009
Mean of IAE				**0.071%**

Table 6 The calculated current and absolute error results for DD model.

Item	V (V)	I (A)	I calculated (A)	IAE
1	-0.2057	0.7640	0.7640	0.0000
2	-0.1291	0.7620	0.7626	0.0006
3	-0.0580	0.7605	0.7613	0.0008
4	0.00057	0.7605	0.7603	0.0002
5	0.0646	0.7600	0.7591	0.0009
6	0.1185	0.7590	0.7581	0.0009
7	0.1678	0.7570	0.7571	0.0001

8	0.2132	0.7570	0.7562	0.0008
9	0.2545	0.7555	0.7551	0.0004
10	0.2924	0.7540	0.7536	0.0004
11	0.3269	0.7505	0.7513	0.0008
12	0.3585	0.7465	0.7472	0.0007
13	0.3873	0.7385	0.7400	0.0015
14	0.4137	0.7280	0.7273	0.0007
15	0.4373	0.7065	0.7070	0.0005
16	0.4590	0.6755	0.6755	0.0000
17	0.4787	0.6320	0.6304	0.0016
18	0.4960	0.5730	0.5725	0.0005
19	0.5119	0.4990	0.4998	0.0008
20	0.5265	0.4130	0.4136	0.0006
21	0.5398	0.3165	0.3172	0.0007
22	0.5521	0.2120	0.2119	0.0001
23	0.5633	0.1035	0.1025	0.0010
24	0.5736	-0.0100	-0.0094	0.0006
25	0.5833	-0.1230	-0.1244	0.0014
26	0.5900	-0.2100	-0.2090	0.0010
Mean of IAE				**0.068%**

Figures 2.4 and 2.5 show the I-V and P-V characteristics for SD and DD models, both simulated and measured data for the RTC France cell at temperature 30 ºC and irradiance 1000W/m^2. They demonstrate that when the solutions yielded by the proposed DE are adopted, both solar cell models can accurately represent the characteristics of the solar cell.

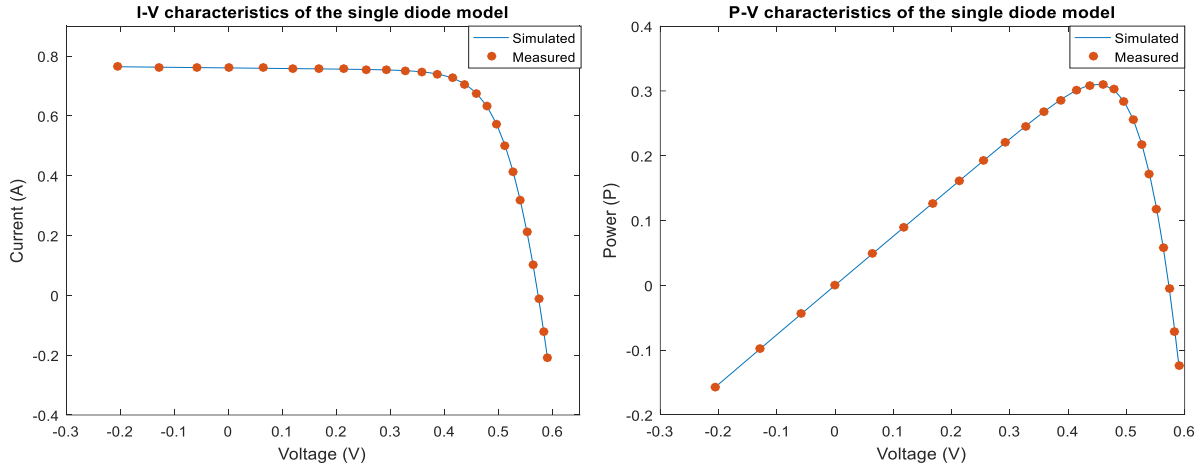

(a) (b)

Figure 2.4 *Comparisons between experimental data and simulated data for single diode model (a) I-V characteristics and (b) P-V characteristics.*

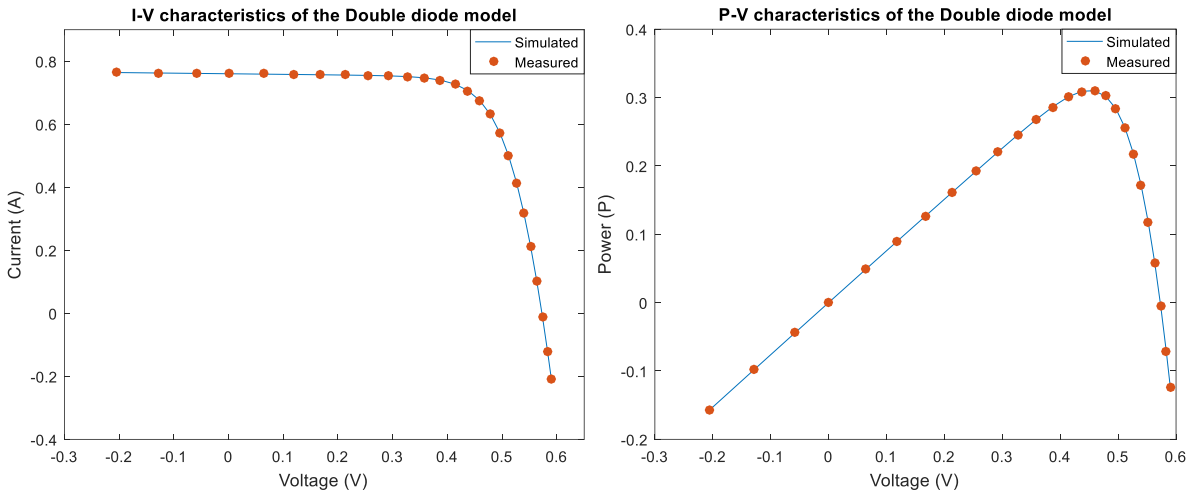

(a) (b)

Figure 2.5 *Comparisons between experimental data and simulated data for double diode model (a) I-V characteristics and (b) P-V characteristics.*

Furthermore, the convergence performance of opposition-based DE for SD and DD models are illustrated in Figure 2.6. From this figure, we can observe that our algorithm, in both models, has fast convergence; it achieved an optimal value before 250 iterations for SD and 500 for DD. In the same context, the proposed DE requires less time to achieve the optimal solutions, for a single run in SD it takes only 52.27 s to extract the unknown parameters and for DD 141.09 s since it is more complex compared to SD.

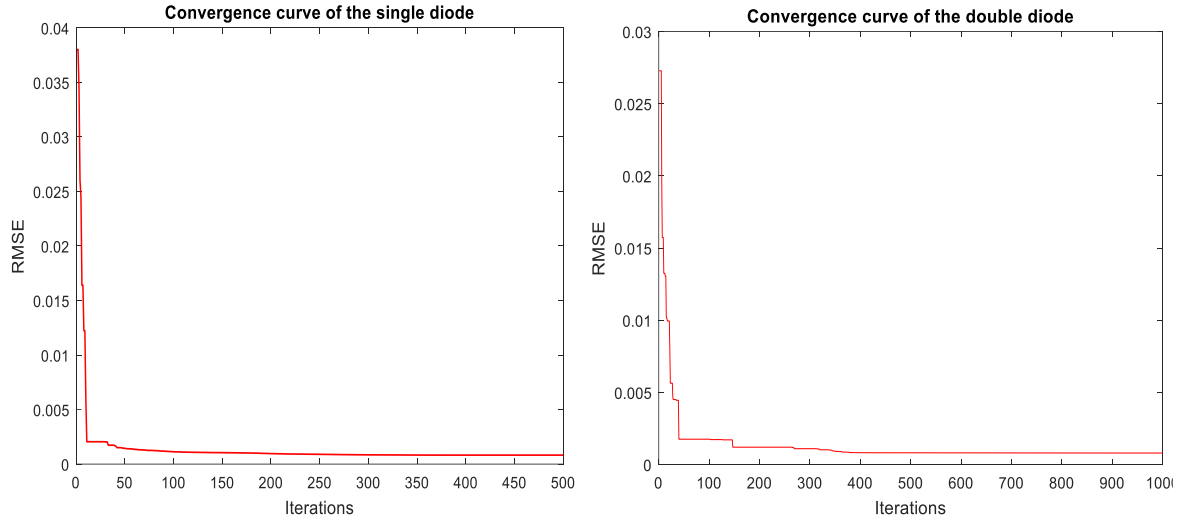

(a) (b)

Figure 2.6 *Convergence curves of (a) SD and (b) DD models.*

Case study #2: Common PV modules

For the PV modules, SD model is used. The 5 parameters and the RMSE values for the polycrystalline module Photowatt-PWP201 which contains 36 cells are presented in Table 7. The current and voltage data were measured at 45ºC. It can be seen that the proposed DE algorithm also obtains the best RMSE value (2.0400×10^{3}) among all algorithms. We can notice that the accuracy in the module is less than the solar cell; this can be explained by the fact that there is always a mismatch between cells and therefore the single diode model for a module will be less accurate than the model of a single cell.

Table 7 Model parameters for the Photowatt-PWP201 module, achieved by different optimisation algorithms.

Algorithm	I_{ph}(A)	I_s(μA)	R_s(Ω)	R_p(Ω)	a	RMSE
Proposed DE	1.0324	2.4966	1.2405	748.3236	1.3166	**2.0400e-03**
DE [7]	1.0305	3.4823	1.2013	981.9819	1.3512	2.4251e-03
Rcr-IJADE [7]	1.0305	3.4823	1.2013	981.9822	1.3512	2.4251e-03
MCSWOA [17]	1.0305	3.4822	1.2013	981.9585	1.3512	2.4251e-03
TLABC [8]	1.0305	3.4823	1.2016	972.9356	1.3509	2.4250e−03

Using the extracted parameters we plotted the I-V and P-V curves for this module, they are presented in Figure 2.7. The simulated curves highly match the measured data which proves the reliability of our algorithm for PV modules as well.

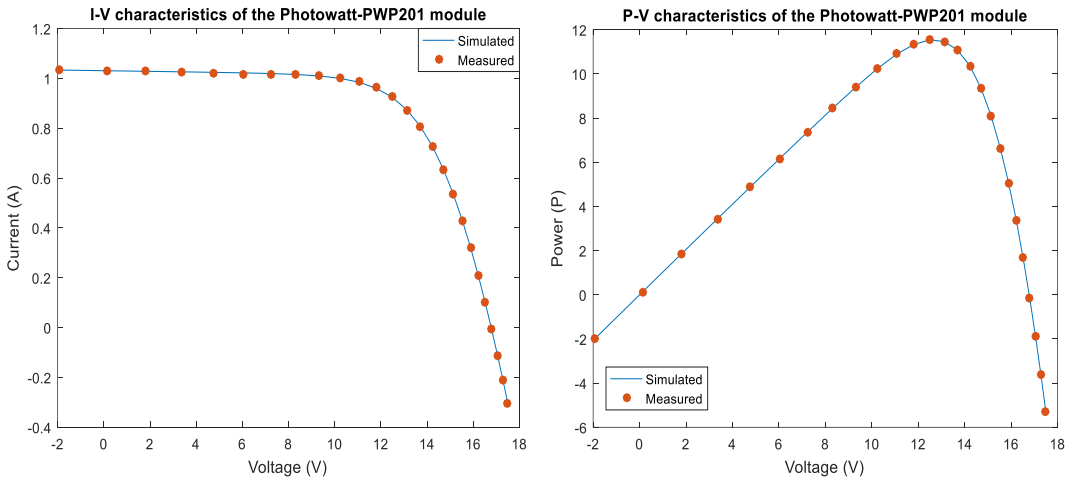

(a) (b)

Figure 2.7 *Comparisons between experimental data and simulated data for the Photowatt-PWP201module (a) I-V characteristics and (b) P-V characteristics.*

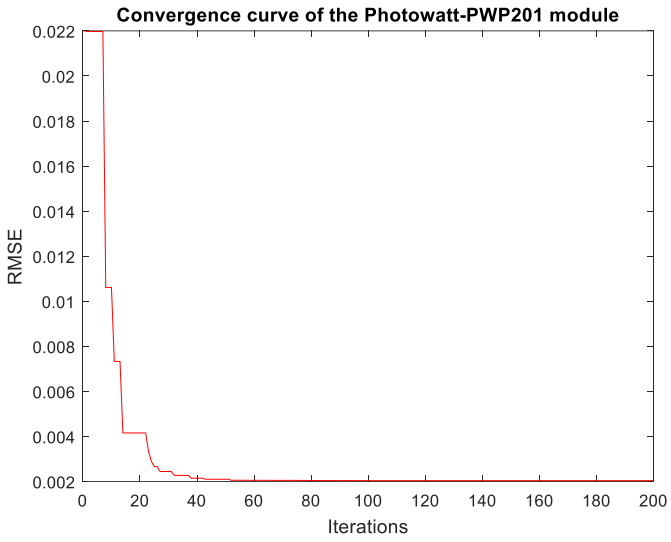

Figure 2.8 *Convergence curve of the Photowatt-PWP201module.*

Figure 2.8 presents the convergence curve for this module; we can notice that the convergence is very fast, the algorithm reaches the optimal solution within 200 iterations in an execution time of 19.9061 s, which again proves the reliability and speed of the proposed DE algorithm.

In Table 8, the measured, calculated current and the individual absolute errors are listed, as we can see the mean absolute error for the Photowatt-PWP201 module is 0.168 % which is very small.

Table 8 The calculated current and absolute error results for Photowatt-PWP201 module.

Item	V (V)	I (A)	I calculated (A)	IAE
1	-1.9426	1.0345	1.0332	0.0013
2	0.1248	1.0315	1.0305	0.0010
3	1.8093	1.0300	1.0282	0.0018
4	3.3511	1.0260	1.0261	0.0001
5	4.7622	1.0220	1.0240	0.0020
6	6.0538	1.0180	1.0219	0.0039
7	7.2364	1.0155	1.0193	0.0038
8	8.3189	1.0140	1.0156	0.0016
9	11.0449	0.9880	0.9846	0.0034

10	11.8018	0.9630	0.9601	0.0029
11	12.4929	0.9255	0.9239	0.0016
12	13.1231	0.8725	0.8736	0.0011
13	13.6983	0.8075	0.8083	0.0008
14	14.2221	0.7265	0.7286	0.0021
15	14.6995	0.6345	0.6367	0.0022
16	15.1346	0.5345	0.5355	0.0010
17	15.5311	0.4275	0.4282	0.0007
18	15.8929	0.3185	0.3178	0.0007
19	16.2229	0.2085	0.2069	0.0016
20	16.5241	0.1010	0.0976	0.0034
21	16.7987	-0.0080	-0.0086	0.0006
22	17.0499	-0.1110	-0.1110	0.0000
23	17.2793	-0.2090	-0.2086	0.0004
24	17.4885	-0.3030	-0.3008	0.0022
Mean of IAE				**0.168 %**

The second and third modules that have been tested are the polycrystalline STP6-120/36, its I-V data were measured at 55 ºC and the monocrystalline STM6-40/36 module measured at 51ºC. Both modules contain 36 cells. Their 5 parameters and RMSE values are presented in Tables 9 and 10. For the STP-120/36, the best RMSE value is reached by the proposed DE (1.4251e-02) and for the STM6-40/36 as well (1.7219e-03).

Table 9 Model parameters for the STP6-120/36 module, achieved by different optimisation algorithms.

Algorithm	I_{ph}(A)	I_s(μA)	R_s(Ω)	R_p(Ω)	a	RMSE
Proposed DE	7.4753	1.9309	0.1689	570.1993	1.2445	**1.4251e-02**
DE [7]	7.4715	2.4257	0.0046	25.2677	1.2633	1.6608e-02
Rcr-IJADE [7]	7.4725	2.3350	0.0046	22.2199	1.2601	1.6601e-02
MCSWOA [17]	7.4727	2.3300	0.0046	21.9831	1.2599	1.6601e-02

Table 10 Model parameters for the STM6-40/36 module, achieved by different optimisation algorithms.

Algorithm	I_{ph}(A)	I_s(μA)	R_s(Ω)	R_p(Ω)	a	RMSE
Proposed DE	1.6639	1.7412	0.1536	573.5339	1.5205	**1.7219e-03**
DE [7]	1.6627	2.3342	0.0033	17.6907	1.5534	1.8669e-03
Rcr-IJADE [7]	1.6639	1.7387	0.0043	15.9283	1.5203	1.7298e-03
MCSWOA [17]	1.6639	1.7390	0.0043	15.9294	1.5203	1.7298e-03

In Tables 11 and 12, the calculated, measured current and the individual absolute error values for both STP6-120/36 and STM6-40/36 modules are listed, the mean errors for these modules are 1.118 % and 0.109% respectively. The accuracy of these values can be seen in the I-V and P-V characteristics curves constructed from the extracted 5 parameters values (Figure 2.9 and 2.10). We can notice that the proposed DE algorithm outperformed the compared algorithms and extracted accurately the 5 parameters for the two types of modules; monocrystalline and polycrystalline.

Table 11 The calculated current and absolute error results for STP6-120/36 module.

Item	V (V)	I (A)	I calculated (A)	IAE
1	19.21	0.00	0.0042	0.0042
2	17.65	3.83	3.8284	0.0016
3	17.41	4.29	4.2708	0.0192
4	17.25	4.56	4.54 38	0.0162
5	17.10	4.79	4.7839	0.0061
6	16.90	5.07	5.0809	0.0109
7	16.76	5.27	5.2733	0.0033
8	16.34	5.75	5.7780	0.0280
9	16.08	6.00	6.0395	0.0395
10	15.71	6.36	6.3515	0.0085
11	15.39	6.58	6.5711	0.0089
12	14.93	6.83	6.8179	0.0121
13	14.58	6.97	6.9612	0.0088
14	14.17	7.10	7.0903	0.0097
15	13.59	7.23	7.2189	0.0111
16	13.16	7.29	7.2845	0.0055

17	12.74	7.34	7.3312	0.0088
18	12.36	7.37	7.3625	0.0075
19	11.81	7.38	7.3945	0.0145
20	11.17	7.41	7.4185	0.0085
21	10.32	7.44	7.4370	0.0030
22	09.74	7.42	7.4446	0.0246
23	09.06	7.45	7.4505	0.0005
24	00.00	7.48	7.4731	0.0069
Mean of IAE				**1.118 %**

Table 12 The calculated current and absolute error results for STM6-40/36 module.

Item	V (V)	I (A)	I calculated (A)	IAE
1	0.0000	1.6630	1.6635	0.0005
2	0.1180	1.6630	1.6633	0.0003
3	2.2370	1.6610	1.6596	0.0014
4	5.4340	1.6530	1.6539	0.0009
5	7.2600	1.6500	1.6506	0.0006
6	9.6800	1.6450	1.6454	0.0004
7	11.5900	1.6400	1.6392	0.0008
8	12.6000	1.6360	1.6337	0.0023
9	13.3700	1.6290	1.6273	0.0017
10	14.0900	1.6190	1.6183	0.0007
11	14.8800	1.5970	1.6031	0.0061
12	15.5900	1.5810	1.5816	0.0006
13	16.4000	1.5420	1.5423	0.0003
14	16.7100	1.5240	1.5212	0.0028
15	16.9800	1.5000	1.4992	0.0008
16	17.1300	1.4850	1.4853	0.0003
17	17.3200	1.4650	1.4656	0.0006
18	17.9100	1.3880	1.3876	0.0004
19	19.0800	1.1180	1.1184	0.0004
20	21.0200	0.0000	0.0000	0.0000
Mean of IAE				**0.109%**

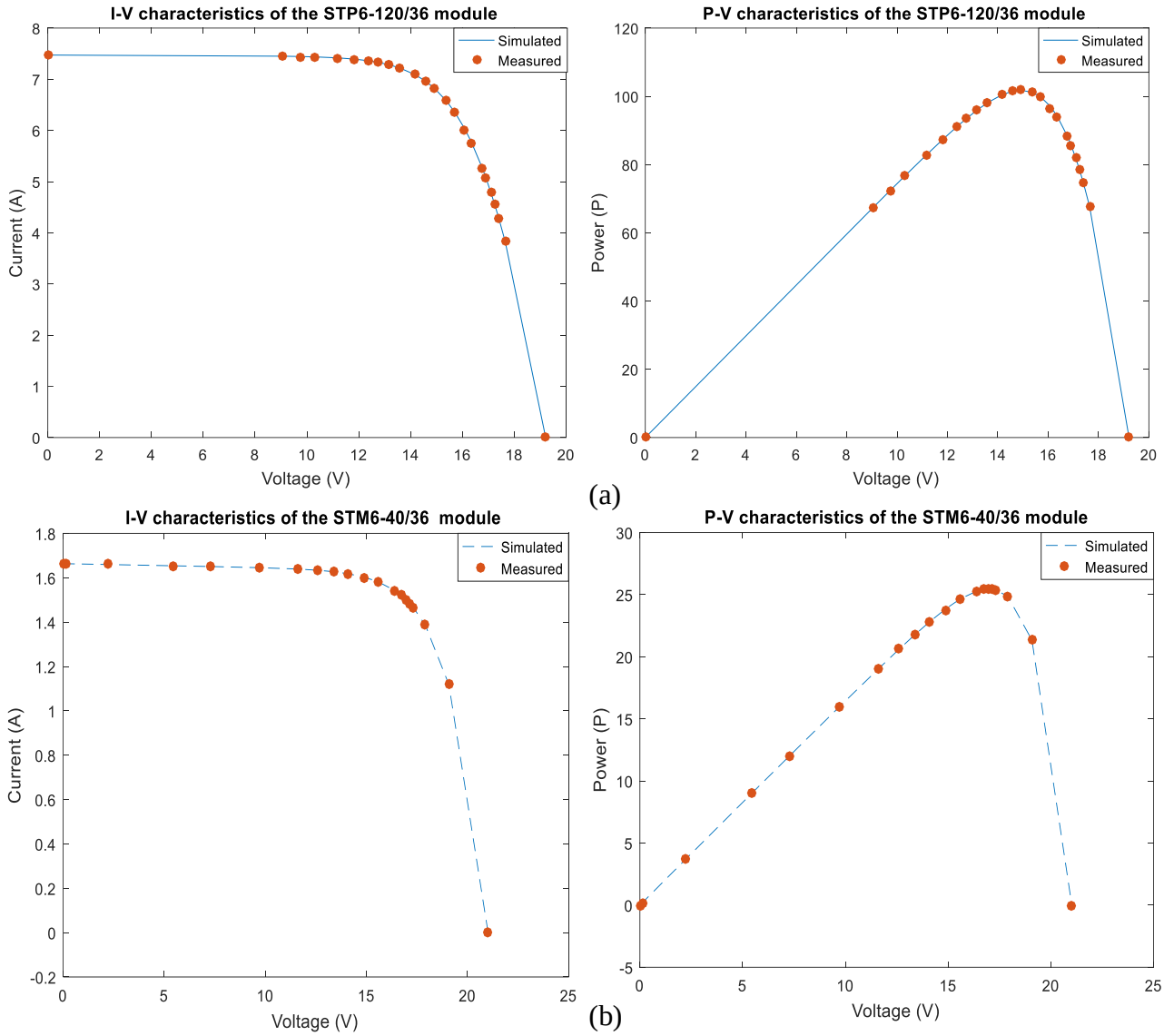

Figure 2.9 *Comparisons between I-V and P-V experimental data and simulated data for (a)* STP6-120/36 *module and (b)* STM6-40/36 *module.*

In Figure 2.10 the convergence curves of both modules are presented, for the STM-40/36 module, the optimal solution is reached within 500 iterations, while the STP6-120/36 within 200 iterations only. That indicates that the proposed DE has a very fast convergence speed.

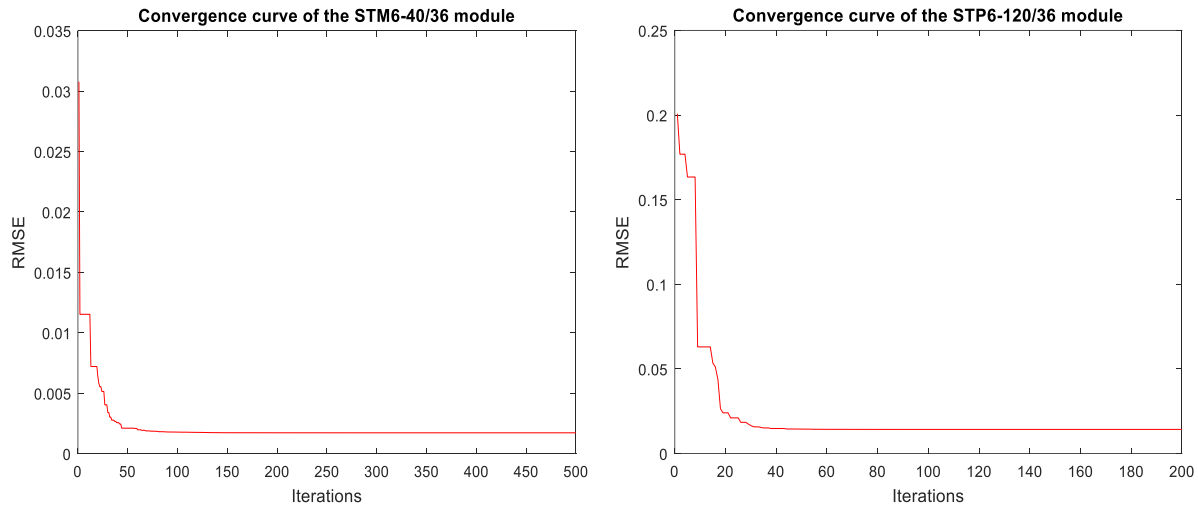

(a) (b)

Figure 2.10 *Convergence curve of (a) STM6-40/36 module, (b) STP6-120/36 module.*

Case Study #3: Other PV modules

Furthermore, the proposed DE is tested on a group of other PV modules which are listed in Table 13. While their parameters and RMSE values are presented in Table 14.

Table 13 Electrical specifications of the PV modules.

Module	Type	Vm (V)	Im (A)	Voc (V)	Ish (A)	Ns	Temp. (°C)
ND-R250A5	Polycrystalline	30.9	8.10	37.6	8.68	60	59.00
KYOCERA 125	Polycrystalline	17.4	7.20	21.70	8.00	36	59.52
SLK60P6L 210	Monocrystalline	28.9	7.3	36.5	8.00	60	57.70
Condor150M	Monocrystalline	18.5	8.11	22.90	8.59	36	53.15

Table 14 Model parameters for the modules, achieved by the proposed DE algorithm.

Module	I_{ph} (A)	I_s (uA)	R_s (Ω)	R_p (Ω)	a	RMSE
ND-R250A5	9.114	0.209	0.643	1500	1.204	1.86e-02
KYOCERA 125	8.008	5.000	0.231	104.454	1.331	2.07e-02
SLK60P6L 210	8.400	0.075	0.470	1500	1.034	8.32e-02
Condor150M	8.318	0.5477	0.2661	1498.96	1.216	1.87e-02

From the results, we observe that the proposed DE provides accurate results with some PV modules (less than 2% with ND-R250A5 and Condor150M) but less accurate with some others (8.32% with SLK60P6L 210). We can also observe that the type of the module does not have an effect on the accuracy, the proposed DE has good results for both monocrystalline and polycrystalline modules.

Convergence Analysis of the 5 parameters:

In order to study the convergence of the 5 extracted parameters, we used the results obtained for the first case (the RTC France solar cell). Figure 2.11 illustrates the convergence curves of the 5 parameters of this solar cell.

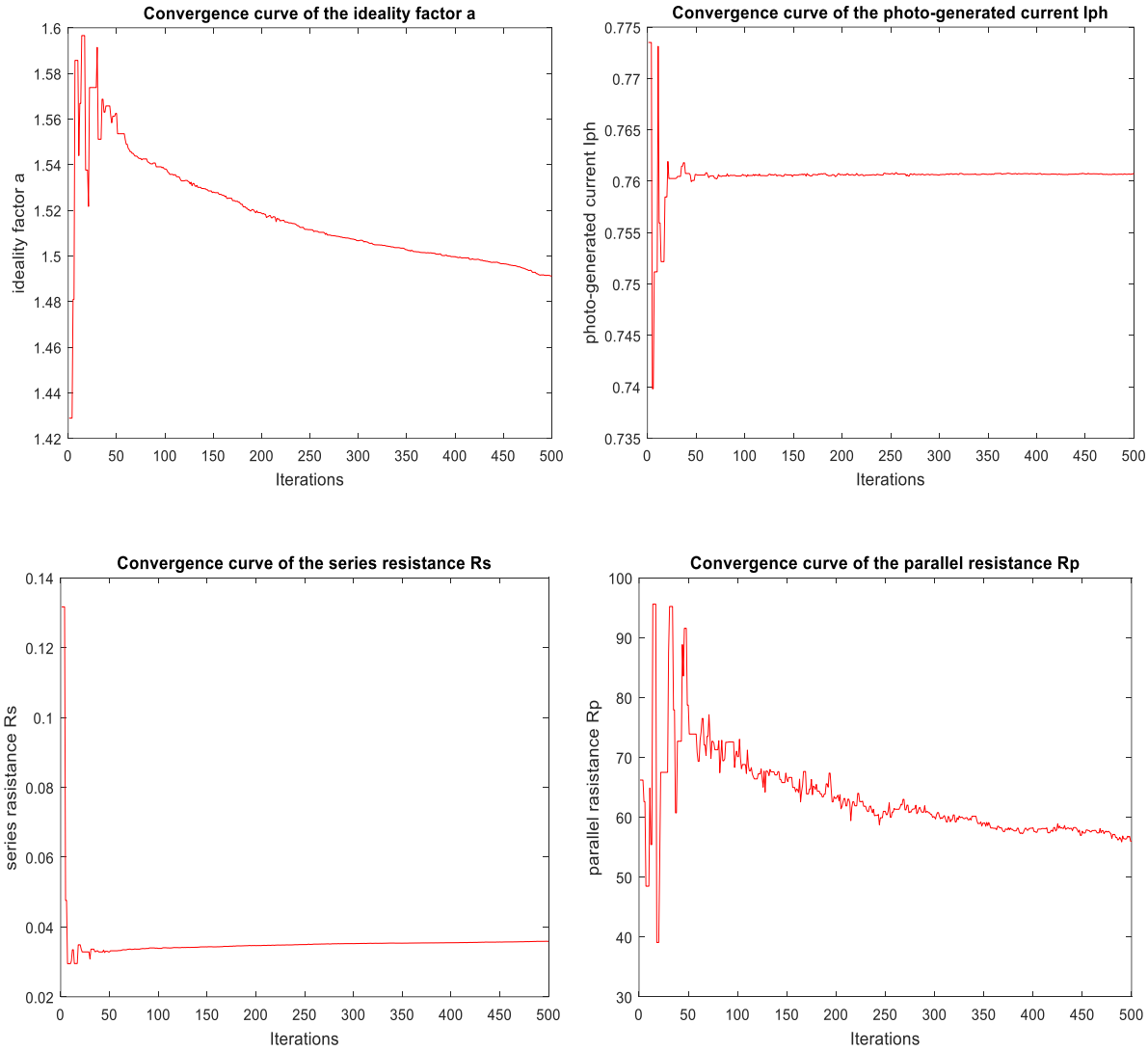

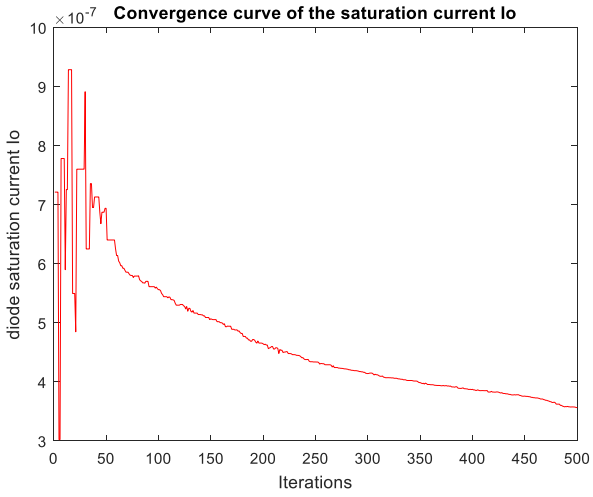

Figure 2.11 *Convergence curves of the 5 extracted parameters for the RTC France solar cell.*

From the figure above, we can observe that some parameters converge faster than others; these parameters are the series resistance and the photo-generated current. This can be explained by the fact that these two parameters are the most sensitive ones in the non-linear I-V equation. In other words, they are the most weighted parameters; any small change in these two will have a remarkable effect on the I-V characteristics.

2.4 Conclusion

In this chapter, Opposition-based DE algorithm was used to extract the parameters of PV cells and modules and was compared to other optimization algorithms. Both SD and DD were used.

The proposed algorithm successfully extracted the parameters with high accuracy and fast speed of convergence, such an algorithm does not need any initial values, and only three parameters need to be set. For the models, we concluded that the DD model is more accurate compared to SD. However, it is more complex and requires more computational time. The algorithm also proved to be effective for different types of modules (monocrystalline and polycrystalline). We conclude that the opposition-based DE is an effective and reliable method to extract the parameters of the PV model.

Chapter 3

Identification of PV parameters based on manufacturer’s data

3.1 Introduction

Optimization methods used in the previous chapter require the experimental current-voltage data in order to identify the parameters of the PV model. Therefore, fast and simplified approaches that calculate all model parameters based only on the data provided by the manufacturer are needed. In this case, no measurements are required. In this chapter, a simple, accurate and fast approach to identify the parameters of the single diode model is presented. This approach is based on the three points that characterize the I-V curve which are the maximum power point, short circuit point and open circuit point. In addition, a novel meta-heuristic method called Black Widow is used in this approach. The algorithm has been tested using MATLAB software on different modules, but can be used on any software or programming environment since it is an iterative algorithm that uses simple equations that are easily solved.

3.2 Proposed Five-Parameters Estimation Method

The first step to develop our method starts from the three points characterizing the I-V curve; these points are used to derive some equations depending on some approximations. Subsequently, using equations from step 1, the values of only three parameters which are Rp, a and Io are then extracted using Black Widow algorithm.

3.2.1 Equations development

The equation used in this step is the single-diode model equation mentioned in chapter 1 (Eq. (9)). When imposing the first condition which is the short circuit condition with $I = I_{sh}$ and V = 0, Eq. (9) becomes:

$$I_{sh} = I_{ph} - I_S\left(e^{\frac{R_S I_{sh}}{a.Vt}} - 1\right) - \frac{R_S I_{sh}}{Rp} \tag{22}$$

Since $Iph \gg I_S\left(e^{\frac{R_S I_{sh}}{a.Vt}} - 1\right)$ and the value of R_s is very low comparing to Rp, and depending on the values obtained in chapter 2; Eq. (22) can be approximated as follows:

$$I_{sh} = I_{ph} \tag{23}$$

Imposing the second condition which is the open circuit condition with I = 0 and V = Voc, Eq. (9) becomes:

$$I_{ph} = I_S\left(e^{\frac{V_{oc}}{a.Vt}} - 1\right) + \frac{V_{oc}}{Rp} \quad (24)$$

Furthermore, Eq. (9) is rewritten as below:

$$V = aV_tLn\left(\frac{I_{ph}+I_s-I-\frac{RsI}{Rp}+\frac{V}{Rp}}{I_s}\right) - R_sI \quad (25)$$

And again imposing the open-circuit condition with I = 0 and V = V_{oc}, Eq. (25) becomes:

$$V_{oc} = aV_tLn\left(\frac{I_{ph}+I_s+\frac{V_{oc}}{Rp}}{I_s}\right) \quad (26)$$

From Eq. (23), we can write Eq. (26) as follows:

$$V_{oc} = aV_tLn\left(\frac{I_{sh}+I_s+\frac{V_{oc}}{Rp}}{I_s}\right) \quad (27)$$

For the last condition which is at the maximum power point with I = Im and V = Vm, we get the following equation:

$$V_m = aV_tLn\left(\frac{I_{ph}+I_s-I_m-\frac{RsI_m}{Rp}+\frac{V_m}{Rp}}{I_s}\right) - R_sI_m \quad (28)$$

The term $\frac{RsI_m}{Rp}$ is very small and can be neglected, so the previous equation becomes:

$$V_m = aV_tLn\left(\frac{I_{sh}+I_s-I_m+\frac{V_m}{Rp}}{I_s}\right) - R_sI_m \quad (29)$$

Subtracting Eq. (29) from Eq. (27) we get the following equation representing the value of the series resistance:

$$R_s = \frac{Voc-Vm+aV_tLn\left(\frac{Ish-Im+Is+\frac{Vm}{Rp}}{Ish+\frac{Voc}{Rp}}\right)}{I_m} \quad (30)$$

- The equations used in the next section to estimate the parameters are Eq. (23), Eq. (24) and Eq. (30). The idea is to use an optimization technique that optimizes only three parameters which are Rp, a and Io by minimizing the error between the approximated value of the photo-generated current (Eq. (23)) and the calculated one (Eq. (24)). Then,

the value of Rs will be calculated using Eq. (30). The optimization technique used in this work is a novel meta-heuristic method called Black Widow [19]. Its process will be presented in the next section.

- The proposed method is shown in Figure 3.1.

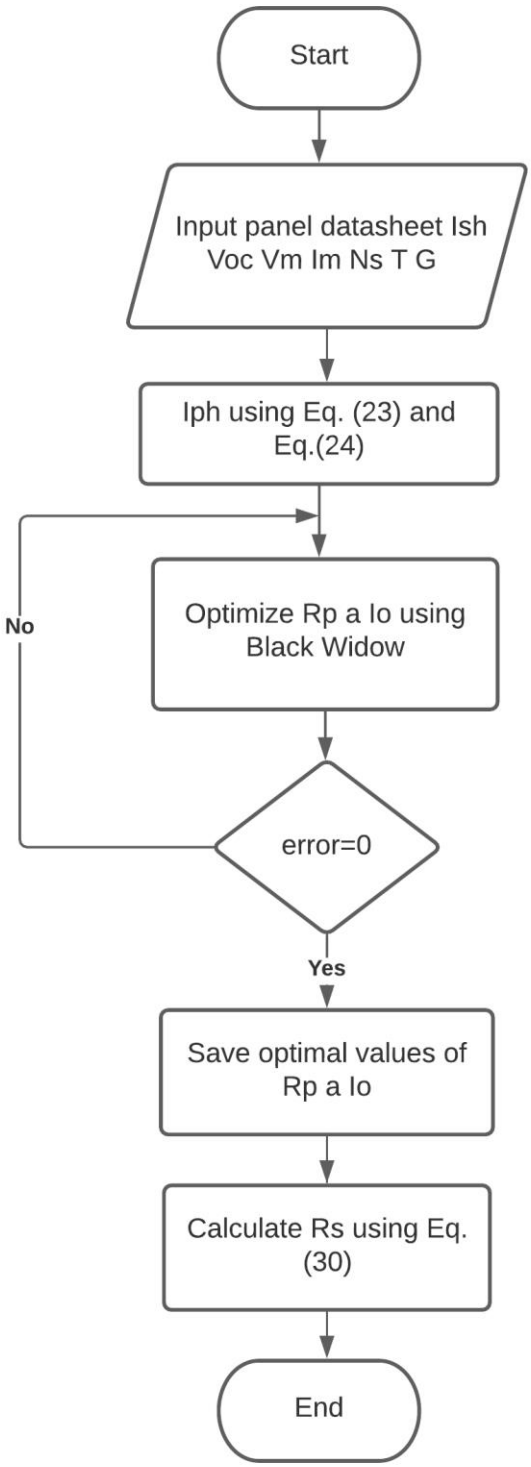

Figure 3.1 *The 5-parameters estimation method.*

- The parameters extraction is conducted for the electrical performance under standard test conditions STC. This method could be extended under varying environmental conditions by using the temperature coefficients of the open-circuit voltage and short-circuit current included in the datasheet. Therefore, the parameters at any temperature and irradiance can be calculated using the following equations [20].

$$I_{ph}(T,G) = \left(I_{ph\,STC} + K_I(T - T_{STC})\right) \times \frac{G}{G_{STC}} \quad (31)$$

$$R_S(T,G) = R_{S\,STC} \times \frac{T}{T_{STC}}\left(1 - 0.217Ln\frac{G}{G_{STC}}\right) \quad (32)$$

$$R_P(T,G) = R_{P\,STC} \times \frac{G_{STC}}{G} \quad (33)$$

$$a(T,G) = a_{STC} \times \frac{T}{T_{STC}} \quad (34)$$

$$I_S(T,G) = I_{S\,STC} \times \left(\frac{T}{T_{STC}}\right)^3 e^{\frac{E_g}{k}\times\left(\frac{1}{T_{STC}} - \frac{1}{T}\right)} \quad (35)$$

Where K_i is the temperature coefficient of the current and E_g is the material's energy bandgap.

3.2.2 Black Widow Optimizer

Black Widow is a population-based optimization algorithm entitled BWO; it is an evolutionary algorithm that imitates the strange mating behaviour of black widow spiders. The female one remains out of sight during the day, and during the night she spins her web. Whenever the female black widow desires to mate, she marks certain spots of her net with pheromone to attract the male. Once a male enters the web, the female consumes it during or post-mating, then she transfers the eggs to her egg sac. A female can lay up to 10 egg sacs, each of which contains about 250 eggs. After hatching the egg, the offspring engages in sibling cannibalism. However, they stay for a short period in their mother's web and they may even consume the mother. This cycle causes survival of the fit and strong individuals. [19]

Figure 3.2 *The black widow spider with her egg sock during hatching.*

The reasons and results of sibling cannibalism are still not well understood. It affects the population-level by reducing the number of surviving spiderlings, but with appended implications for the general fitness of the cannibal and its parents. Spiderlings that eat their mother can have very good survival rates than the ones that do not.

3.2.2.1 Black Widow Algorithm

Like other evolutionary algorithms, BWO starts with an initial population of spiders, each spider represents a solution. These spiders try to reproduce the new generation. Then the individuals enter a loop of 4 stages. It is suitable for continuous nonlinear optimization problems and it converges very fast comparing to other algorithms.

- **Initial Population:** Each black widow spider shows the values of the problem variables. Therefore, they should be considered as arrays of $1 \times D$ where D is the dimension of the problem (number of variables)**.** Widow = $[x_1, x_2 \ldots x_D]$

  To start the optimization algorithm, a candidate widow matrix of size $NP \times D$ is generated.

  $$X_{i,j} = L_j + (H_j - L_j) \times \text{rand}(0, 1) \qquad j = 1, 2 \ldots D \tag{36}$$

- **Procreate:** In this step**,** each independent individual starts to mate in order to reproduce the new generation, here in the algorithm in order to reproduce, an array called alpha should be randomly created. Then offspring is produced by using α with the following equation.

  $$\begin{cases} y_1 = \alpha \times x_1 + (1 - \alpha) \times x_2 \\ y_2 = \alpha \times x_2 + (1 - \alpha) \times x_1 \end{cases} \tag{37}$$

  Where x_1 and x_2 are parents from the population, y_1 and y_2 are offspring, the reproduction rate RP determines the number of reproduction NR according to Eq. (38).

  $$NR = \text{round}(RP \times NP / 2) \times 2 \tag{38}$$

- **Cannibalism:** There are three types of cannibalism; the first one is sexual cannibalism, in which the female eats her husband during or after mating. In the algorithm, we can recognize male and female by their fitness functions.

  Another kind is sibling cannibalism, in which the strong spiderlings eat the weaker ones. In the algorithm, we set a cannibalism rate CR according to which the number of survivors is determined. While the third kind is when baby spiders eat their mother. Again we use fitness function to determine strong and weak spiders.

- **Mutation:** In this stage, a number of individuals NM are selected and they exchange two elements in the array. This number is calculated depending on the mutation rate MR using Eq. (39).

  $$NM = \text{round}(MR \times NP) \quad (39)$$

  The pseudo code of the black widow algorithm is presented below.

Algorithm 2: The main procedure of BWO

Input: Control parameters: rate of procreating, rate of cannibalism, rate of mutation.
Output: Optimal solution.

Initialization: Generate random population P of NP spiders of D dimension using Eq. (36).
For G = 1 to Gmax do
Calculate number of reproduction NR using Eq. (38).
Select the best NR solutions and save them.
Procreating and cannibalism:
For i = 1 to NR do
Select parents and generate offspring using Eq. (37).
Destroy father.
Based on CR destroy some children.
Save solutions.
End for.
Mutation:
Calculate NM using Eq. (39).
For i = 1 to NM do
Select a solution and randomly mutate it with another.
Save the new one.
End for.
Return Best solution.
End procedure.

3.2.2.2 Objective function

Like any optimization algorithm, an objective function should first be set. In our project and in order to optimize the parameters Rp, a and Io, the fitness function used is the absolute error

between the approximated photo-generated current and the calculated one which can be defined as follows:

$$\begin{cases} F(X) = I_S\left(e^{\frac{V_{oc}}{a.Vt}} - 1\right) + \frac{V_{oc}}{Rp} - Ish \\ X = \{a, R_p, I_s\} \end{cases} \quad (40)$$

Then, the fitness function is defined:

$$f = |F(X)| \quad (41)$$

3.3 Results and Discussion:

In this section, the proposed method is applied to extract the parameters of the single diode model. The algorithm is tested on some PV modules and compared with two methods to prove its effectiveness. Experimental data for these modules are used for comparison.

The algorithm is implemented in MATLAB R2016a and all simulations are executed on a PC with Intel(R) Celeron(R) N3050 processor @ 1.60GHz 1.60GHz, 4GB RAM, under the Windows 8 64-bit OS.

The search ranges for the three parameters to be optimized are the same used in the previous chapter. Number of iterations used is 250. The datasheets of the modules used are presented in Table 15. Regarding the experimental settings of the BWO, they are presented in Table 16.

Table 15 Datasheets of the PV modules.

Module	Type	Vm	Im	Voc	Ish	Ns	STC (T/G)
ND-R250A5	Polycrystalline	30.9	8.10	37.6	8.68	60	25 / 1000
KC200GT	Polycrystalline	26.3	7.61	32.9	8.21	54	25 / 1000
SLK60P6L 210	Monocrystalline	28.9	7.3	36.5	8.00	60	25 / 1000
Condor150M	Monocrystalline	18.5	8.11	22.90	8.59	36	25 / 1000

T**able 16** Parameter settings of the proposed method.

Parameter	value
Reproduction rate PR	0.8
Mutation rate MR	0.2
Cannibalism rate CR	0.2
Population NP	50

Case study #1: KC200GT module at STC

The polycrystalline module KC200GT is used in this part, and the results are compared with two other methods. The absolute error between the calculated current and the measured one [21] is used for the evaluation. Table 17 presents the parameters extracted using the proposed method while Table 18 presents the mean absolute errors obtained. The errors presented by both models are plotted on the same graph (Figure 3.3).

T**able 17** The 5-parameters extracted using the proposed method.

Parameter	value
I_{ph} (A)	8.2100
I_s (µA)	2.9325
R_s(Ω)	0.1188
R_p(Ω)	823.5460
a	1.5979

T**able 18** Mean absolute errors for the different methods.

Parameter	MAE
Proposed method	7.59 %
Villalva [22]	17.80 %
Walker [23]	32.46 %

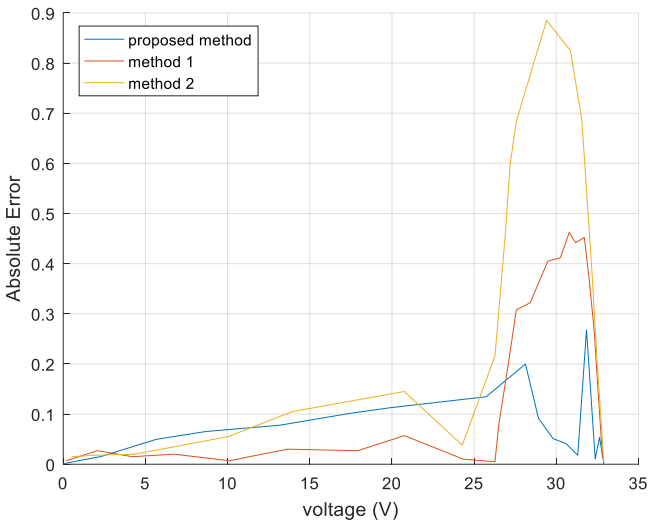

Figure 3.3 *Absolute errors of the model proposed in this work and in* [22-23] *for the Kyocera KC200GT solar array at 25◦C, 1000 W/m2.*

As can be seen from Table 18 and the curves in Figure 3.3, the mean absolute error obtained by the proposed method (7.59%) is better than the two other methods which proves the effectiveness of this technique in extracting the unknown PV parameters. In addition, the convergence using this method is very fast, where the execution time was only 3.6178 s.

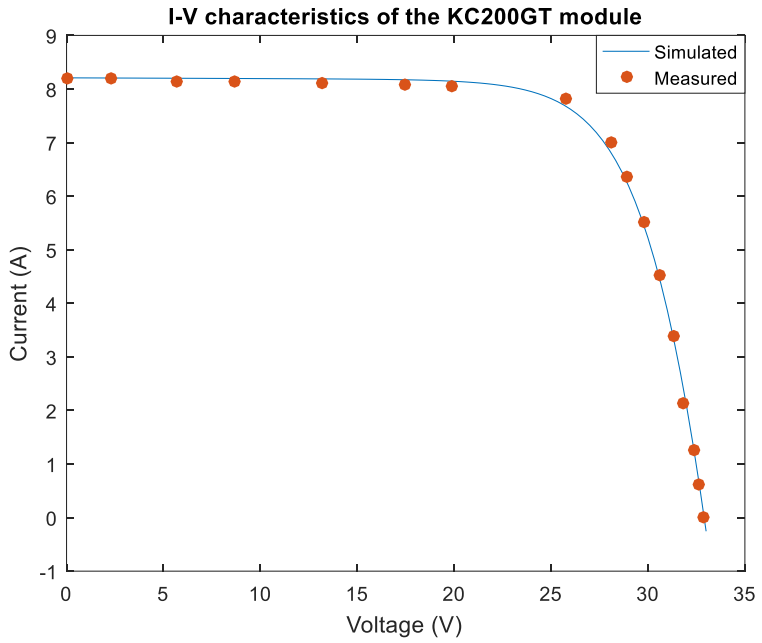

Figure 3.4 *Comparison between experimental data and simulated data of the I-V characteristic of the KC200GT module.*

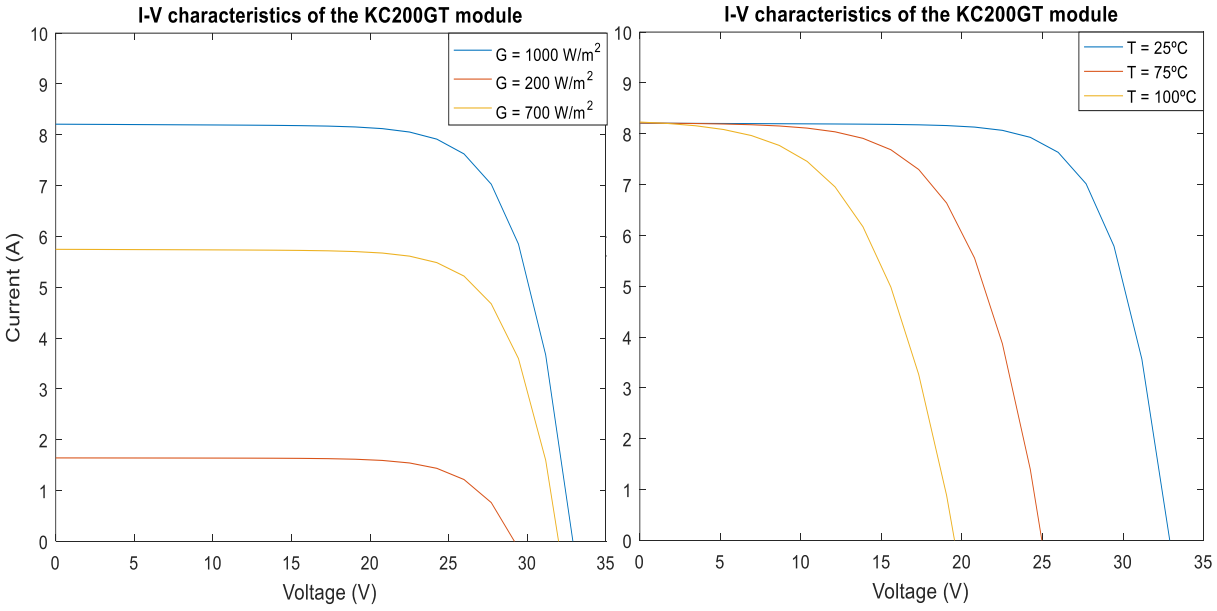

Figure 3.5 *I-V curves of the KC200GT module at different temperatures and irradiances.*

Furthermore, in order to prove how accurate the model is, the I-V curve is constructed using the extracted parameters and compared with the experimental data as shown in Figure 3.4. Using Eq. (31-35), the parameters of the module at different temperatures and irradiances were extracted from the STC ones and the simulated curves are shown in Figure 3.5; they confirm the effect of temperature on the open circuit voltage where at high temperatures, the voltage is reduced. And for the irradiance, its effect is mostly on the short circuit current where its value increases at high irradiance values.

Case study #2: PV modules at different temperature and irradiance

In this section, the three modules: ND-R250A5, SLK60P6L 210 and Condor150M are tested. Using their datasheets at STC, their parameters will be extracted. Then, using the equations (31-35), the parameters at different temperature and irradiance will be extracted. In Table 19, the temperature and irradiance that the modules were tested at are mentioned. Then, Table 20 presents the values of the extracted parameters at STC while Table 21 at the mentioned temperatures and irradiances.

Table 19 Temperature and irradiance of the PV modules.

Module	Temperature (°C)	Irradiance (W/m^2)
ND-R250A5	59.00	1040.00
SLK60P6L 210	57.70	1026.50
Condor150M	53.15	877.66

T**able 20** The 5-parameters extracted at STC using the proposed method.

Parameter	ND-R250A5	SLK60P6L 210	Condor150M
I_{ph} (A)	8.6800	8.000	8.5900
I_s (μA)	3.1780	3.6093	3.0602
R_s (Ω)	0.0030	0.2240	0.0035
R_p (Ω)	617.4327	1131.9	682.6937
a	1.6466	1.6093	1.6679

T**able 21** The 5-parameters extracted at different temperature and irradiance using the proposed method.

Parameter	ND-R250A5	SLK60P6L 210	Condor150M
I_{ph} (A)	9.2120	8.4983	8.3100
I_s (µA)	0.0124	0.0165	0.0169
R_s (Ω)	0.4500	0.2421	0.0044
R_p (Ω)	1000	2000	622.1232
a	1.7614	1.7526	1.8230

The proposed technique extracted the parameters of the PV single diode model accurately for both STC conditions and other conditions.

Figure 3.6 shows the simulated I-V curves as well as the measured values for the three modules, the blue curves represent the simulated I-V curves at STC conditions, while the orange curves are the simulated curves obtained after extracting the parameters at the given conditions. Depending on the results we obtained, we can say that this technique extracts the parameters at STC with very good accuracy. However, for other conditions, using Eq. (31-35) the extraction is less accurate, but still gives a good model that can be used in designing PV systems.

(a)

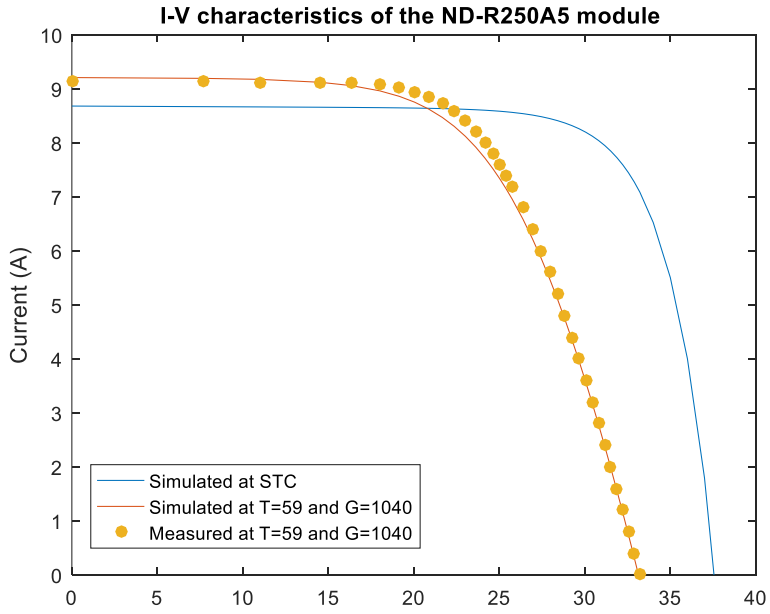

(b)

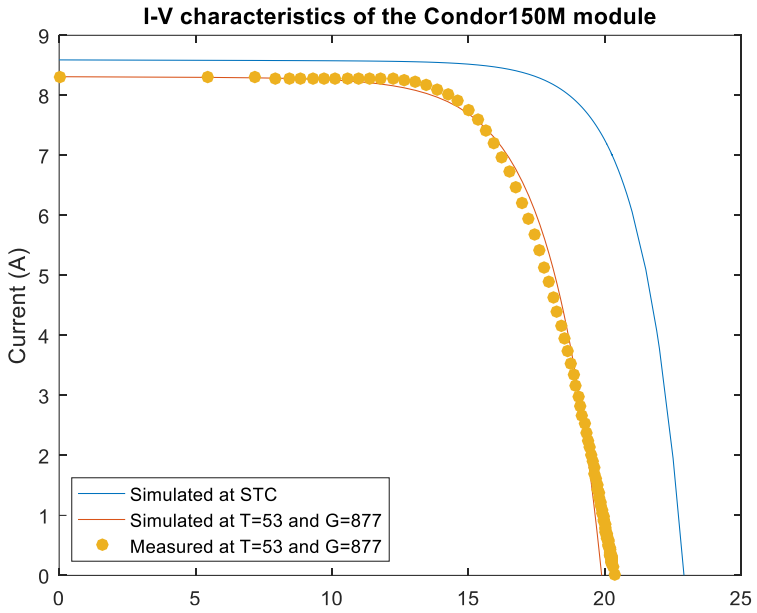

(c)

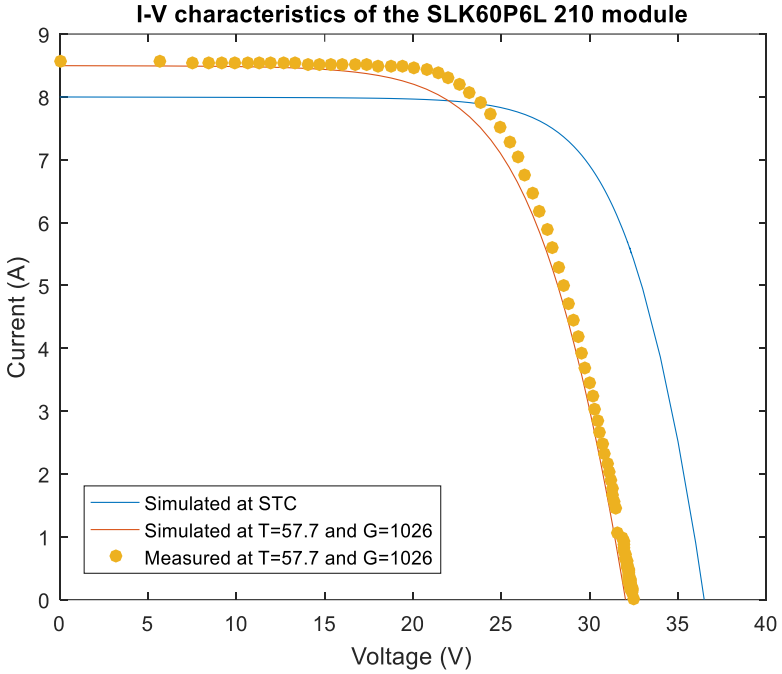

Figure 3.6 *Comparison between experimental and simulated curves of: (a) ND-R250A5, (b) Condor150M and (c) SLK60P6L 210.*

3.4 Conclusion

In this chapter, a novel technique was used to extract the parameters of PV modules based only on manufacturer's datasheet and was compared to other methods. The single diode model was used.

The proposed method successfully extracted the parameters with acceptable accuracy and fast speed of convergence. The method also proved to be effective for different types of modules (monocrystalline and polycrystalline). We conclude that the proposed method is an effective and reliable method to extract the parameters of the PV model and can be used later to design PV systems.

General Conclusion

Estimating an accurate model for the PV modules is central to the design, manufacturing and evaluation of PV systems as it permits to forecast the behaviour of systems under different working conditions.

Obtaining the most accurate five parameters model was the main objective of this project. In this work, we first covered the main principles of PV systems. In the second part, we identified the parameters of both single diode and double diode models using an optimization algorithm developed based on DE and opposition-based learning, it used the I-V data acquired from the PV modules. This improvement made on DE makes the algorithm inherits the strength property of DE; in addition, it saves the computational time that may be needed. Our proposed algorithm showed a satisfying estimation as the five parameters were extracted with minimum errors. In the third part, the five parameters of the single diode model were extracted based on the datasheet provided by manufacturers using a new technique based on BWO that proved to be quite good and accurate.

Finally, after the proposed methods were tested by using a dataset of experimental values of several modules, we can say that the main purpose of this work is well achieved as we solved the photovoltaic design problem by estimating the parameters of solar cells and modules.

The output characteristics of current and voltage in the PV system are closely related to the solar irradiance, ambient temperature and wind speed during the real operation process Therefore, future work will include designing a new improved N-diode PV model in consideration of these all environmental factors through real measurement experiments. In addition, the accuracy of the second method can be improved by developing equations for the double diode model. Furthermore, attempts will be made to apply the proposed methods to solve maximum power point tracking (MPPT) problems.

Bibliography

[1] “Types of Photovoltaic Cells.” Types of photovoltaic cells - Energy Education. Accessed June 10, 2021. https://energyeducation.ca/encyclopedia/Types_of_photovoltaic_cells.

[2] Ndegwa, Robinson, Justus Simiyu, Elijah Ayieta, and Nicodemus Odero. “A Fast and Accurate Analytical Method for Parameter Determination of a Photovoltaic System Based on Manufacturer’s Data.” Journal of Renewable Energy 2020 (2020): 1–18.

[3] Stornelli, Muttillo, de Rubeis, and Nardi. “A New Simplified Five-Parameter Estimation Method for Single-Diode Model of Photovoltaic Panels.” Energies 12, no. 22 (2019): 4271.

[4] Orioli, Aldo, and Alessandra Di Gangi. “A Procedure to Calculate the Five-Parameter Model of Crystalline Silicon Photovoltaic Modules on the Basis of the Tabular Performance Data.” Applied Energy 102 (2013): 1160–77.

[5] Shongwe, S., and M. Hanif. “Gauss-Seidel Iteration Based Parameter Estimation for a Single Diode Model of a PV Module.” 2015 IEEE Electrical Power and Energy Conference (EPEC), 2015.

[6] Yetayew, T. T., and T. R. Jyothsna. “Parameter Extraction of Photovoltaic Modules Using Newton Raphson and Simulated Annealing Techniques.” 2015 IEEE Power, Communication and Information Technology Conference (PCITC), 2015.

[7] Yang, Xi, Wenyin Gong, and Ling Wang. “Comparative Study on Parameter Extraction of Photovoltaic Models via Differential Evolution.” Energy Conversion and Management 201 (2019): 112113.

[8] Chen, Xu, Bin Xu, Congli Mei, Yuhan Ding, and Kangji Li. “Teaching–Learning–Based Artificial Bee Colony for Solar Photovoltaic Parameter Estimation.” Applied Energy 212 (2018): 1578–88.

[9] Omar, Abeer Shaban, Hany M. Hasanien, Ahmed Al-Durra, and Walid H. El-Hameed. “Water Cycle Algorithm for Parameters Estimation of Solar Photovoltaic Model.” International Journal on Energy Conversion (IRECON) 7, no. 3 (2019): 117.

[10] Ye, Meiying, Xiaodong Wang, and Yousheng Xu. “Parameter Extraction of Solar Cells Using Particle Swarm Optimization.” Journal of Applied Physics 105, no. 9 (2009): 094502.

[11] Tchoketch_Kebir, Selma. “Study of a New Hybrid Optimization-Based Method for Obtaining Parameter Values of Solar Cells.” IntechOpen, 2020. Available: https://www.intechOpen.com/onlinee-first/study-of-a-new-hybrid-optimization-based method-for-obtaining-parameter-values-of-solar-cells.

[12] Jones, Andrew E., and G. W. Forbes. “An Adaptive Simulated Annealing Algorithm for Global Optimization over Continuous Variables.” Journal of Global Optimization 6, no. 1 (1995): 1–37.

[13] Rivera-Lopez, Rafael, and Juana Canul-Reich. “Differential Evolution Algorithm in the Construction of Interpretable Classification Models.” Artificial Intelligence - Emerging Trends and Applications, (2018) (pp.49-73) First Edition.

[14] Rahnamayan, Shahryar, Hamid R. Tizhoosh, and Magdy M.A. Salama. “A Novel Population Initialization Method for Accelerating Evolutionary Algorithms.” Computers & Mathematics with Applications 53, no. 10 (2007): 1605–14.

[15] Oliva, Diego, Ahmed A. Ewees, Mohamed Abd Aziz, Aboul Ella Hassanien, and Marco Peréz-Cisneros. “A Chaotic Improved Artificial Bee Colony for Parameter Estimation of Photovoltaic Cells.” Energies 10, no. 7 (2017): 865.

[16] Rezaee Jordehi, A. “Enhanced Leader Particle Swarm Optimisation (ELPSO): An Efficient Algorithm for Parameter Estimation of Photovoltaic (PV) Cells and Modules.” Solar Energy 159 (2018): 78–87.

[17] Xiong, Guojiang, Jing Zhang, Dongyuan Shi, Lin Zhu, Xufeng Yuan, and Gang Yao. “Modified Search Strategies Assisted Crossover Whale Optimization Algorithm with Selection Operator for Parameter Extraction of Solar Photovoltaic Models.” Remote Sensing 11, no. 23 (2019): 2795.

[18] Fathy, Ahmed, and Hegazy Rezk. “Parameter Estimation of Photovoltaic System Using Imperialist Competitive Algorithm.” Renewable Energy 111 (2017): 307–20.

[19] Hayyolalam, Vahideh, and Ali Asghar Pourhaji Kazem. “Black Widow Optimization Algorithm: A Novel Meta-Heuristic Approach for Solving Engineering Optimization Problems.” Engineering Applications of Artificial Intelligence 87 (2020): 103249.

[20] Jordehi, A. Rezaee. “Parameter Estimation of Solar Photovoltaic (PV) Cells: A Review.” Renewable and Sustainable Energy Reviews 61 (2016): 354–71.

[21] Abdelqawee, I. M., Ayman Y. Yousef, Khaled M. Hasaneen, H. G. Hamed, and Maged N. F. Nashed. “Determination of Unknown Parameters of Photovoltaic Module Using Genetic Algorithm.” Indonesian Journal of Electrical Engineering and Computer Science 4, no. 2 (2016): 271-278.

[22] Villalva, M.G., J.R. Gazoli, and E.R. Filho. “Comprehensive Approach to Modeling and Simulation of Photovoltaic Arrays.” IEEE Transactions on Power Electronics 24, no. 5 (2009): 1198–1208.

[23] G. Walker, “Evaluating MPPT converter topologies using a matlab PV model,” J. Elect. Electron. Eng., Australia, vol. 21, no. 1, pp. 45–55, 2001.

[24] S., DU, KE-LIN. SWAMY, M. N. SEARCH AND OPTIMIZATION BY METAHEURISTICS: Techniques and Algorithms Inspired by Nature. BIRKHAUSER, 2018.

[25] Park, Jun-Young, and Sung-Jin Choi. “A Novel Simulation Model for PV Panels Based on Datasheet Parameter Tuning.” Solar Energy 145 (2017): 90–98.

[26] Ulapane, Nalika N., Chamari H. Dhanapala, Shyama M. Wickramasinghe, Sunil G. Abeyratne, Nimal Rathnayake, and Prabath J. Binduhewa. “Extraction of Parameters for Simulating Photovoltaic Panels.” 2011 6th International Conference on Industrial and Information Systems, 2011.

[27] Humada, Ali M., Mojgan Hojabri, Saad Mekhilef, and Hussein M. Hamada. “Solar Cell Parameters Extraction Based on Single and Double-Diode Models: A Review.” Renewable and Sustainable Energy Reviews 56 (2016): 494–509.

[28] Han, Wei, Hong-Hua Wang, and Ling Chen. “Parameters Identification for Photovoltaic Module Based on an Improved Artificial Fish Swarm Algorithm.” The Scientific World Journal 2014 (2014): 1–12.